

DESIGN OF A CONTROL SYSTEM FOR AN ELBOW JOINT MOTION SIMULATOR

by

Patrick J. Schimoler

B.S. in Mechanical Engineering, University of Pittsburgh, 2005

Submitted to the Graduate Faculty of
The Swanson School of Engineering in partial fulfillment
of the requirements for the degree of
Master of Science in Mechanical Engineering

University of Pittsburgh

2008

UNIVERSITY OF PITTSBURGH
SWANSON SCHOOL OF ENGINEERING

This thesis was presented

by

Patrick J. Schimoler

It was defended on

March 31, 2008

and approved by

Daniel D. Budny, Ph. D., P.E., Associate Professor, Department of Civil and Environmental
Engineering

Mark C. Miller, Ph. D., Associate Research Professor, Department of Mechanical Engineering
and Materials Science

Jeffrey S. Vipperman, Ph. D., Associate Professor, Department of Mechanical Engineering
and Materials Science

Thesis Advisor: Jeffrey S. Vipperman, Ph. D., Associate Professor, Department of
Mechanical Engineering and Materials Science

Copyright © by Patrick J. Schimoler

2008

DESIGN OF A CONTROL SYSTEM FOR AN ELBOW JOINT MOTION SIMULATOR

Patrick J. Schimoler, M.S.

University of Pittsburgh, 2008

An elbow joint motion simulator provides the ability to derive various measures from cadaveric elbow specimens such as the kinematic effects of radial head prostheses and ligament strains. To ensure that the data collected is meaningful, the system must be able to actuate the elbow through chosen displacements in a repeatable manner. A control system is developed in this thesis capable of performing this task. Linear positioners which create motion by applying loads through the brachialis, triceps, biceps, and pronator teres move the arm through flexion / extension or pronation / supination movements. Sensors measure loading and displacement states enabling the use of proportional-integral-derivative feedback control. Results indicate the system's capability. Suggestions for future work are given.

TABLE OF CONTENTS

1.0	INTRODUCTION	1
1.1	MOTIVATION.....	1
1.2	GOALS	1
2.0	LITERATURE REVIEW	3
2.1	1950'S – 1970'S	3
2.2	1980'S.....	7
2.3	1990'S.....	11
2.4	2000'S.....	16
3.0	METHODS	19
3.1	FEEDBACK REALIZATION WITH AVAILABLE HARDWARE	19
3.1.1	Elbow Frame.....	19
3.1.2	Controller and Breakout Box	20
3.1.3	Actuators.....	20
3.1.4	Sensors	23
3.1.5	Sensors for System Protection	25
3.2	PID CONTROL.....	27
3.2.1	Discrete PID Algorithm	27
3.3	SOFTWARE IMPLEMENTATION.....	29
3.3.1	Control Requirements	29

3.3.2	Flexion / Extension Controller.....	29
3.3.3	Evolution of the Full Controller Design	34
3.3.4	Programmable Logic Controller for Limit Switches	38
4.0	RESULTS AND DISCUSSION	44
4.1	PERFORMANCE MEASURES	44
4.2	FLEXION / EXTENSION CONTROLLER	47
4.3	FINAL CONTROLLER	53
4.3.1	F/E at Constant P/S Angle	54
4.3.2	P/S at Constant F/E Angle	59
4.3.3	Preliminary Concurrent Motions	64
4.4	KEY LIMITATIONS	67
5.0	CONCLUSIONS AND FUTURE WORK	71
5.1	ACCOMPLISHMENTS	71
5.2	FUTURE WORK.....	72
	APPENDIX A. CONTROLLER CODE.....	73
	APPENDIX B. CONTROLLER TESTING RESULTS.....	88
	BIBLIOGRAPHY.....	91

LIST OF TABLES

Table 1. Performance of F/E controller displacement feedback with various triceps loading	88
Table 2. Performance of F/E controller force feedback with various triceps loading	88
Table 3. Performance of F/E controller as triceps loads are varied	88
Table 4. Performance of F/E controller as biceps and pronator teres minimum loads are varied	89
Table 5. Performance of F/E controller as P/S angle is varied	89
Table 6. Performance of P/S controller as F/E angle is varied	89
Table 7. Performance of P/S controller as the biceps and pronator teres minimum loads are varied.....	89
Table 8. Performance of P/S controller at various F/E angles	90
Table 9. Performance of controller during a concurrent F/E and P/S motion	90

LIST OF FIGURES

Figure 1. Comparison of dynamic and wear testing JMS's	8
Figure 2. Illustration of the hardware arrangement to perform P/S	25
Figure 3. Illustration of the hardware arrangement to perform F/E.....	26
Figure 4. Limit switch output relative to ballscrew position	27
Figure 5. Muscles used for F/E controller	30
Figure 6. Block diagram for F/E controller	32
Figure 7. Determining load and displacement control in the F/E controller	33
Figure 8. Muscles used for P/S control.....	35
Figure 9. Effect of switch on a sine wave	37
Figure 10. Block diagram of P/S controller	38
Figure 11. PLC or / and configurations	40
Figure 12. PLC latch signals.....	40
Figure 13. Move killing limit switch PLC	42
Figure 14. Jog killing limit switch PLC.....	42
Figure 15. Two sine waves offset by a constant lag	45
Figure 16. Cross correlation of the two sine waves	46
Figure 17. Successful removal of lag from two sine waves	46
Figure 18. Maintenance of correct flexion angle during F/E tests.....	48
Figure 19. Maintenance of correct triceps tension during F/E tests	48

Figure 20. Plots of the three F/E trials with a triceps load of 4 LBS	50
Figure 21. Plots of the three F/E trials with a triceps load of 16 LBS	50
Figure 22. Plots of the triceps loads during three trials with a triceps reference load of 4 LBS ..	51
Figure 23. Plots of the triceps loads during three trials with a triceps reference load of 16 LBS	51
Figure 24. Plots of the brachialis loads during three trials with a triceps reference load of 4 LBS	52
Figure 25. Plots of the brachialis loads during three trials with a triceps reference load of 16 LBS	52
Figure 26. Improvement in triceps load control due to proportional gain increase	53
Figure 27. Maintenance of various P/S angles during F/E	55
Figure 28. Effects of minimum biceps and pronator teres loads on P/S tracking.....	56
Figure 29. Examples of various constant P/S angles during F/E tests.....	56
Figure 30. F/E tracking while holding various P/S angles constant	57
Figure 31. Loading in brachialis tendon during F/E.....	57
Figure 32. Biceps loads during a typical F/E trial	58
Figure 33. Pronator Teres loads during a typical F/E trial.....	59
Figure 34. Effects of varying the F/E angle on maintaining a constant F/E angle during P/S	60
Figure 35. Constant F/E angle during P/S trials	61
Figure 36. Effects of minimum biceps and pronator teres load on biceps load control	62
Figure 37. P/S tracking at various constant F/E angles	62
Figure 38. Typical biceps loads during a P/S trial.....	63
Figure 39. Typical pronator teres loads during a P/S trial	64
Figure 40. Displacement control performance of concurrent motion controller	65
Figure 41. Concurrent F/E and P/S displacement.....	66

Figure 42. Loading in biceps tendon during concurrent motion..... 66

Figure 43. Pronator teres loads during concurrent motion 67

Figure 44. Bit status and encoder position versus time along with the derivative of the encoder position..... 68

Figure 45. Bit status and encoder position versus time along with the derivative of the encoder position..... 68

Figure 46. Illustration of the variable length of control cycles due to the inability to control an interrupt..... 70

NOMENCLATURE

θ_F – Flexion Angle
 θ_{F_R} – Flexion Reference Angle
 θ_P – Pronation Angle
 θ_{P_R} – Pronation Reference Angle
F/E – Flexion / Extension
JMS – Joint Motion Simulator
 K_D – Derivative Gain
 K_I – Integral Gain
 K_P – Proportional Gain
 L_B – Biceps Load
 L_{B_R} – Biceps Minimum Load
 L_{Br} – Brachialis Load
 L_{Br_R} – Brachialis Reference Load (Minimum)
 L_{PT} – Pronator Teres Load
 L_{PT_R} – Pronator Teres Minimum Load
 L_T – Triceps Load
 L_{T_R} – Triceps Reference Load
PID – Proportional / Integral / Derivative
PLC – Programmable Logic Controller
P/S – Pronation / Supination
 T_D – Derivative Time Constant
 T_I – Integral Time Constant
 V_B – Biceps Actuator Velocity
 V_{Br} – Brachialis Actuator Velocity
 V_{PT} – Pronator Teres Actuator Velocity
 V_T – Triceps Actuator Velocity

1.0 INTRODUCTION

1.1 MOTIVATION

Healthy elbow function enables various integral parts of daily life to be taken for granted such as eating, bathing, and a multitude of pick and place activities. Because of its importance, the health of the elbow must be maintained and, in the case of injury, restored. Severe elbow injury, e.g. a comminuted fracture, can lead to the insertion of a radial head prosthesis. Studies have shown the post-operative satisfaction with radial head implants is less than that of other implants [1]. During serious elbow injuries, ligaments may be damaged, increasing the importance of the radial head in stabilizing the elbow.

A testbed, known as a joint motion simulator (JMS), capable of performing testing would also provide a means for testing ligament strains as well as control algorithms to further enhance the knowledge of the body's control of the elbow. It is clear that a system capable of elucidating the kinematic effects of a prosthesis is valuable in a number of ways.

1.2 GOALS

The elbow joint motion simulator is being designed to further research along two avenues. The first revolves around clinical goals. Current demands are to provide a system capable of

performing two different, but related movements: a flexion / extension (F/E) movement at a constant pronation / supination (P/S) angle for the testing of elbow ligament strains and a P/S movement at a constant F/E angle for determining kinematic differences between the native radial head and various prosthetic radial heads.

The second avenue concerns long-term neuromuscular control. Little is known about the control of the elbow. The ability to apply various control schemes and then compare the states to those measured in the body can provide indications of similarities between the body and the generated schemes. This system is not intended to provide those comparisons directly, but instead to provide proof that the system is capable of feedback control and provide a foundation for research that will provide those comparisons.

2.0 LITERATURE REVIEW

Because of academic and clinical interests in biomechanics, joint motion simulators have been developed for the study of various joints. The following sections describe the history and control methodologies used in previously designed JMS's.

Although active control was not used with the earliest systems, it is worthwhile to review them as they provide the foundation for more recent simulators and illustrate the shortcomings that drove the development of actively controlled simulators.

2.1 1950'S – 1970'S

As far back as the 1950s, systems were already being developed that show commonalities with current simulators. In 1953 [2], Hicks developed a system that described the changes in the shape of the foot under load, confirmed the already described axes of rotation, and determined those axes which were previously unknown. Like most current simulators, a bone proximal to the body part or joint to be studied was fixed rigidly in the simulator allowing for some means of physiologic actuation, in this case, the tibia. This allowed loads to be applied which simulated the application of body weight while standing. Interestingly, the platform the foot rested on could be shifted relative to the load applied [3]; this simulated the ability of the foot to be off balance and provided further visual feedback in assuring physiologic load application. Free

weights and spring systems in conjunction with pulleys were used to apply loads up to 200 pounds to the tendons. Such a system lent itself to simple load variations, but those loads could only be constant dead weights.

The next wave of simulators started in the early 1970s with two knee simulators. Shaw and Murray [4] produced a knee simulator in hopes of developing an intermediate safety measure between prosthesis development and clinical implantation. Their paper was designed to be a “guideline for the development of other simulators by other laboratories.” They listed the yieldable results as the testing of range of motion, prosthesis wear and lifespan, and joint stability. They were explicit in stating that the simulator was only an approximation of the in vivo environment making it unable for certain qualifications such as the body’s tolerance for a poorly sized prosthesis or mechanical behavior due to bone growth around the prosthesis. Although an early paper on the subject of simulators, it included one of the clearest, most practical views of what a JMS could and could not accomplish. Shaw and Murray also provided details on a knee simulator they built to analyze the importance of prosthesis orientation errors. Metal tubing provided a socket for the insertion of the femur and tibia providing a means to fix a leg section with the knee prosthesis into the simulator. This two socket system would be standard among wear testers which provide more constraint than more physiologic dynamic JMS’s that would appear later. Loading, simulating the hip, was provided by dead weights added to the femoral socket. Between the load and socket there was a universal joint which allowed the load distribution to be chosen by the user making simulations of improper implantation possible. The socket for the tibia represented the ankle joint. It could move in the sagittal plane allowing the flexion and extension of the ankle due to flexion and extension at the knee. It could also rotate in a lateral-medial plane. An active hydraulic cylinder provided

loading similar to the quadriceps enabling the flexion and extension of the knee. Valves controlled by a relay logic circuit provided means to control cycle speed, rotation limits, and other unnamed cycle characteristics. This paper was very important as it was the first example of a simulator with some sort of active feedback control with switches that marked range of motion limits and fed back a signal to reverse direction.

Only months after the report by Shaw and Murray, Swanson et al. released a paper that described a wear tester [5], one of the major types of JMS's, for knee and hip implants. It was desirable to have a system which could perform cyclic loading and provide a means to examine the corrosion products released during normal use, as they could be toxic to the body. By providing a temperature controlled bath that surrounded the implanted prosthesis, Swanson et al. were able to collect all of the metal flakes released during testing. It was important for wear testers to not only control the loading applied, but also the surrounding environment of the prosthesis as that factored into the aging as well. Tests were typically run at approximately 1 Hz, slightly below the system's maximum speed, driven by a 750 watt electric motor capable of applying cyclic or constant loads on the order of a half ton. Forces and moments in the joint were constantly recorded so that the frictional forces and moments on the prosthesis could be calculated.

In 1977, Zachman [6] wrote a thesis at Purdue University on a dynamic knee simulator known as the "Accuflexor" which was capable of actuating a knee in motions like walking, stair ascending, and stair descending. It was designed like a slider crank with the hip being the slider, the tibia the crank, and the femur, the connecting rod. The system allowed the application of four loads and would serve as a popular design in knee JMS's. The first load was along the axis of movement of the slider or hip. The second was a load applied from the upper leg around the

knee to the tibia emulating a quadriceps load. The third was a moment that could rotate the tibia. The fourth was a load which could mimic sliding the foot medially or laterally. A mixture of load and force control was used to ensure the hydraulic actuators moved the system under the desired loads through the desired motions. The system was used for both wear testing and elucidation of the kinematics of bodies around the joint with different prostheses. This second goal marked another major type of knee simulator, the dynamic simulator, designed to monitor the effects of prostheses on movement relative to the native case. The Purdue simulator has been modified and redesigned numerous times up until the present and articles and theses chronicling these developments are easy to find.

In 1979, another wear tester was presented by Pappas and Buechel [7], the New Jersey Knee Simulator. They ran flexion cycles at slightly over 1 Hz with a knee which was periodically loaded with a mechanical cam. Loading patterns could only be changed with the changing of the cam, this was beneficial in terms of repeatability, but poor in terms of system flexibility. These two concerns would be major factors in the movement towards computer controlled systems which could provide both features. Similar to Swanson et al., the knee was submerged in a temperature controlled bath.

Over these three decades few simulators were built, but the progression shown in only these four reported was significant. Hicks' system was an array of pulleys and levers used to applied dead weight loads to a cadaveric specimen. At the other end of the spectrum was the simulator designed at Purdue which actively applied loads with a mixture of force and displacement control. Also among these four systems could be found the two general types of JMS's: non-physiologic wear testers and physiologic dynamic simulators.

2.2 1980'S

In the 1980s, joint motion simulators included more active control. The prominence of knee JMS development continued.

In the summer of 1980, Rastegar et al. [8] detailed an ankle simulator driven by a hydraulic drill press. Loads were applied through a drill press-like mechanism to the lower leg. A dynamometer, rigidly attached to the foot, could determine loads and moments transmitted through the ankle to the foot. Multiple degrees of freedom at the point of load application and lack of ankle constraint allowed the ankle's axis of rotation to settle into its position of least resistance. This prevented non-physiologic motions. This was also the first system to involve a computer in some capacity, in this case for data acquisition.

Treharne et al. [9] developed another knee replacement wear tester in 1981 to test various prostheses. In order to enable high loading and fast response a computer controlled hydraulic system was developed. Load cells and linear variable differential transducers (LVDTs) were used for feedback. Because it was computer controlled, it was easier to apply various load profiles in contrast to a cam driven simulator like that of Pappas and Buechel. To produce the most robust results, loading profiles were chosen based on the worst cases reported in the literature, another technique that would become common. In some respects, wear simulators had to encompass more physiologic qualities than a dynamic simulator because the environment of the human body also had to be simulated. A temperature controlled bath filled with calf serum helped to mimic the frictional environment and to add or remove heat as needed. Like the Purdue simulator, this system was ahead of its time as it was fully computer controlled and illustrated the benefits with its speed, accuracy, and adjustability. A comparison of typical

characteristics of both dynamic JMS's and wear testing JMS's is provided by Figure 1 to summarize.

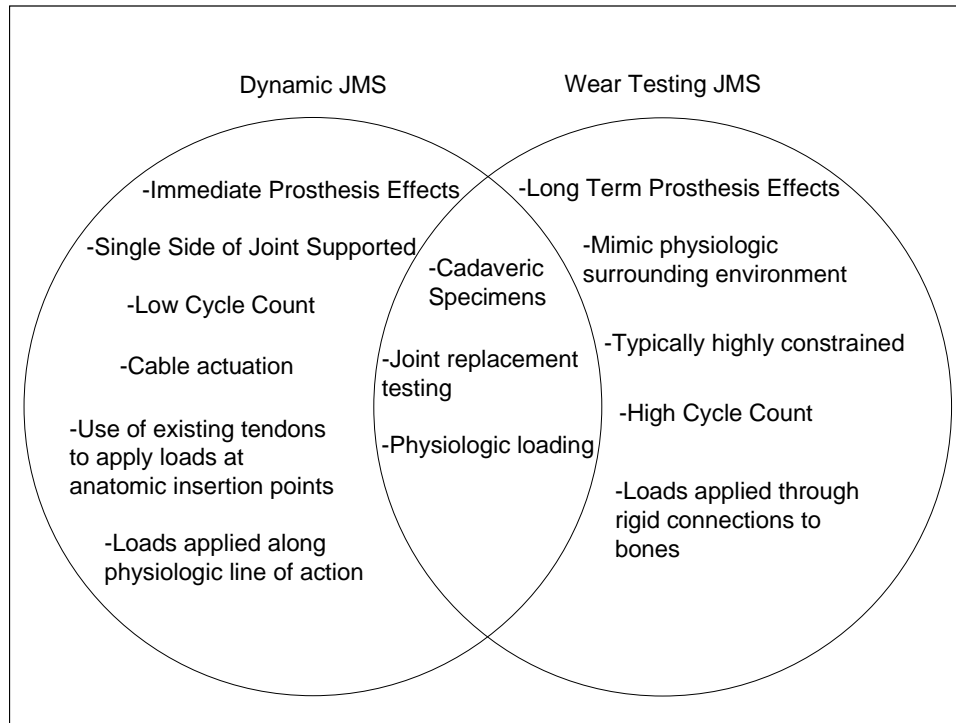


Figure 1. Comparison of dynamic and wear testing JMS's

In 1983, Ahmed and Burke [10] developed a knee simulator with the goal of measuring the static pressure distribution on the tibial surface. The simulator allowed the application of various compressive or shear loads as well as torques on the joint over a range of knee flexion angles from full extension to 90° of flexion. Actuation was hydraulic with no mention of control system design.

Tong [11] developed a wrist joint motion simulator at the University of Syracuse. The system was able to control F/E and radial / ulnar deviation with four hydraulic actuators. The primary movers in the system were driven by signals calculated from a kinematic model.

Displacement feedback was used to minimize model error and load control of antagonists was used to provide stability. Years later, the system was expanded to include nine actuators by Gillison [12]. This system was important as it was an early example of a model-based control system.

In 1987, Ensberg [13] produced one of the last simulators without active control in an effort to study the effects of loading an ankle in various orientations. The system allowed the application of medial / lateral, anterior / posterior, and inferior loads to a lower leg / foot specimen which could be oriented in any configuration due to a gimbaled frame design.

Also in 1987, Szklar and Ahmed [14] published a paper detailing the design of a new unconstrained dynamic knee simulator. This simulator allowed the study of the knee's dynamic response so that soft tissues strains as well as relative motion of the bodies of the knee joint could be studied. Although unconstrained, the system was only actuated in flexion and extension. Two cables were used, one as a flexor and one as an extensor. This approximation of a group of muscles with one actuator was extremely common throughout the literature. The servo hydraulic system employed ran at approximately 1.25 Hz. The system managed the actuator redundancy by moving both in unison, a precursor to later systems which would mimic agonist / antagonist co-activation. Load feedback was provided by pressure transducers. A unique system was used to feed back velocity. Specimen specific transfer functions were derived relating the hydraulic ram position to knee angle. Years later, McLean and Ahmed [15] updated this simulator to be able to apply forces simulating a foot to floor reaction that was independent of the rest of the loads.

Around the same time, Cain et al. developed a system to study anterior stability of the glenohumeral joint [16]. The rig provided a rigid attachment for the scapula and for pulleys

which directed forces along physiologic lines of action. The system was built inside of an Instron machine which was used to apply an external rotation moment to the humerus through movement of the crosshead. A potentiometer attached to the axis of rotation of the humerus provided external rotation data quantifying the stability due to various weights hung from the rotator cuff. Like most systems of this time, it was developed with a mixture of dead weights and feedforward control. Similar to Rastegar et al., an existing piece of test equipment with valuable features was adapted to form a JMS.

In 1988, Lewis et al. [17] detailed a knee joint simulator designed for measuring ligament strains and joint motion. An unconstrained tibia was actuated by cables tensioned by pneumatic actuators while the femur was fixed. Moments could be applied about the tibia and loads could be applied compressively to the joint and anteriorly to the tibia. Feedback was used to ensure the loads were applied as desired. The F/E plane of the knee was parallel to the ground making gravitational forces orthogonal to the F/E axis. A counterbalance system removed the gravitational effects that still loaded the knee. This system was unique in that only loads applied by the simulator acted on the system; compensation was provided for all gravitational loads.

In summary, the 1980s saw the development primarily of knee JMS's. The use of computer controlled data acquisition became standard. Computer control became much more prominent mostly because of its ability to simplify the application of loading and displacement patterns. Neither feedback control nor the use of some sort of agonist / antagonist co-activation was standard.

2.3 1990'S

The development of joint motion simulators in the 1990s continued what started in the 1980s; the vast majority of systems moved to active control with much more closed-loop feedback.

Berns et al. [18] developed a knee JMS to test the flexibility of the knee. Unlike all previous knee simulators, this system actually fixed the flexion angle so that flexibility about the other degrees of freedom could be determined at different flexion angles. Initially the system could only perform testing at flexion angles between full extension and 45°. Bach and Hull [19] would later improve the system to apply loads over the knee's entire physiologic range of motion. Specific loads along the unconstrained degrees of freedom were applied through the use of closed-loop load control. There were two types of loading application used in the design: single loads and paired loads. Single load application was a matter of single-loop feedback. Interestingly, an intentional 10% overshoot produced a more constant load because stretching prevented creep from occurring later. Paired load application was more complicated and used a type of adaptive algorithm. It was desired to maintain the same muscle loading ratio throughout the test. The adaptive algorithm was used because the loads increase nonlinearly and model-based uncertainty made accurate feedforward control unrealistic. Stepper motors were driven by constant computation of the difference between the current loading ratio and the desired loading ratio.

In 1992, DiAngelo et al. [20] debuted a hip JMS capable of loading the hip at various femoral flexion angles. This enabled the testing of various internal fixation methods of the acetabulum, the cup-like part of the pelvis that contacts the femur. The system was able to provide cyclic loading with maximum forces of 550N applied axially to the femur. This JMS

was significant as it was a variation on the wear tester in which cyclic loading was used to test the stability of a fixation method as opposed to the degradation of a prosthesis.

In 1993 [21], King et al. described a system which provided the foundation for the development of elbow joint motion simulators up to the present time. Due to the inconsistency of post surgical satisfaction with total elbow arthroplasty, the authors built a system capable of testing the stability of elbows under simulated muscle loading. Their primary goal was the comparison of the Norway Elbow implant to the native case. A jig was created that secured the humerus and provided routing for cables which connected the biceps, brachialis, and triceps tendons to dead weights. The arm was typically oriented such that weights attached to the distal forearm hung straight down simulating varus or valgus loads. The addition of more muscles and different types of active control to this setup covers the progress that has been made in elbow joint motion simulator development. The work of King et al. is interesting in two respects. First, it is one of the first reported elbow JMS's and lays the foundation for later elbow JMS's. Second, its design reinforces the trend in which the first simulator for a joint is without active control with subsequent integration of active control.

MacWilliams et al. [22,23,24] developed a simulator at Johns Hopkins University for the comparison of native and replaced knees. The system was able to control either load or displacement for actuators simulating the hip position, quadriceps muscles, or hamstrings muscles. The system was fully computer controlled. A similar system was also designed by Pavlovic et al. [25] except the horizontal position of the ankle was also under closed-loop control, providing the ability to vary foot position in the medial / lateral and anterior / posterior directions.

Wuelker et al. [26] designed a shoulder simulator in 1995 that provided more active control than the system designed by Cain et al. Pneumatic actuators applied controlled loads to the deltoid and rotator cuff. Loading ratios between the muscles were derived from relationships between cross sectional area of the muscles. The resulting orientation of the arm was measured by six ultrasonic sensors.

Debski et al. [27] from the University of Pittsburgh also developed a shoulder JMS. Physiologic scapula motion could be created relative to the thorax with six degrees of freedom. Forces up to 670 N were able to be applied through six servo-actuated, hydraulic cylinders. The actuators were arranged to apply forces mimicking the rotator cuff muscles and the middle deltoid. Electronic circuitry provided a choice between displacement and load control on each actuator. Load cells and LVDTs provided force and displacement feedback, respectively, from all of the cylinders. Future plans for the simulator included the addition of a model which would be able to calculate input profiles for desired motions. This system added the option of displacement or force control on each actuator and involved more muscles than previous simulators.

Just as systems evolved from passive loading to computer controlled loading and finally to closed-loop feedback control; the next step in JMS evolution may be the introduction of feedforward models within closed-loop feedback control. By considering existing lags and movement speeds, Stroeve [28] has shown that the body must combine feedforward and feedback control.

A wrist JMS was developed by Werner et al. [29] of the State University of New York Health Science Center. The dynamic simulator was designed to examine the function of the wrist tendons. Servohydraulic actuators were used to apply loads to six tendons in the wrist.

The loads applied were measured using strain gages. A three degree of freedom goniometer was used to measure the angular displacement of the hand. Both step like and cyclic motions were performed. In all cases, force feedback was provided on muscles deemed antagonists in order to provide joint impedance and smooth the motion, while the primary movers were operated under displacement control. This simulator was significant for two reasons. The small movements of the wrist provide the smallest scale movement of all the JMS's and required fine control. In addition, six actuators were the largest number used in this means of agonist / antagonist co-contraction in the literature.

After a number of years without a new system, Walker et al. [30] introduced another knee prosthesis wear tester. This system was designed to be able to run millions of cycles as the authors felt it was important to measure wear into at least the second decade of usage which could entail 30 million cycles. Perhaps more important than the simulator itself was the conclusion that it was best to have a system in which the load was specified instead of the displacement. This design point yielded wear testers that were robust to varying prosthesis shape, which otherwise would have required unique displacement profiles.

Around the same time, Burgess et al. [31] published their work on a servo hydraulic six station knee wear simulator. The ability in and of itself to test six knees at one time was novel and provided an important feature for long term testing that can take months. Also interesting were the authors' comments on the dynamic wear tester versus the classic wear tester in which the specimen was constrained on both sides of the joint. The authors believed the dynamic simulators were not sufficiently robust for the megacycle testing required to predict the long term wear behavior of a prosthesis.

Sharkey and Hamel [32] from Penn State University developed a foot JMS with the hopes of being able to create a realistic loading environment of the stance phase of gait. All actuators involved in the simulator were driven with closed-loop force control. The force profiles used to drive the feedback loops were developed from EMG measurements. The magnitudes of these profiles were scaled to each other by comparing observed peak tensions. Therefore, one muscle's peak tension needed to be specified and from there the rest could be calculated, in this case the tension for the triceps surae was specified. Interestingly, the common problem of controller computational power was solved by offloading some of the computational work of force feedback to separate electronics in the form of microcontrollers. This modular approach was unique and practical for load controlled systems whose only job was to maintain a given tension.

One of the last simulators to be designed in the 1990s was that of Li et al. [33] from the University of Pittsburgh. To the author's knowledge this was the first system to use a 6 DOF robot to actuate a specimen. The femur was fixed with the robot driving the tibia through a 6 DOF load cell. Loads required to maintain the leg at different angles with the ACL present were measured and recorded. The ACL was then resected and through comparison to the normal case, it was possible to determine the forces in the ACL.

Over the course of the 1990s, computer control became the norm for JMS's; the transition from passively loaded static mechanisms was complete. Knee simulators were still the most prominent, but simulators now also existed for shoulders, elbows, wrists, ankles, and hips.

2.4 2000'S

JMS's in the new millennium combined the advances of the past century and were completely computer controlled taking advantage of closed-loop feedback. In terms of this thesis, the most important work was published from the University of Western Ontario on an elbow JMS during this time.

Johnson et al. [34] chronicled the development, implementation, and importance of an elbow joint motion simulator. Their goal was to produce an elbow joint motion simulator that could produce repeatable forearm and wrist motion during flexion-extension or pronation-supination. Five muscles were put under load control in their simulator: biceps, brachialis, brachioradialis, pronator teres, and triceps. The simulator was designed in such a way as to provide physiologic lines of action for the applied forces. Physiologic loading was ensured by considering both EMG activity and cross-sectional area of real muscles. By comparing the multiplication of these two measurements, it was possible to create loading ratios between the muscles. These loading ratios were then used at levels near the minimum possible to produce motion. These minimum levels were found through an iterative process starting with loads incapable of generating motion. The study clearly showed that repeatability was increased with the use of an active JMS over passive actuation, where passive in this case meant the movement of a specimen by a human technician. A 30.6% reduction in variability was shown with the use of active control during F/E tests of 120°. In addition to repeatable trials, the system also benefited from the stability provided by the added joint impedance of the antagonistic loading.

Dunning et al. [35] went on to investigate the effects of loading levels on repeatability. It was found that the presence of active control, not the actual load levels used, was the key factor

in repeatability. This importance was exacerbated for unstable elbows in which innate joint stability was lowered by cutting the Lateral Collateral Ligament.

Further advancement of the elbow motion simulator was provided by Dunning et al. Displacement control was added to the force control [36]. The brachialis and biceps were designated 'primary movers' and were displacement controlled, allowing the other three previously mentioned muscles to operate under load control. Linear resistive transducers (LRTs) were used to provide the displacement feedback to a PID controller handled by LabVIEW. This mixture of displacement and force control made it possible to control velocity and joint impedance in a much simpler manner than possible with pure force control which required a very accurate model.

Still prominent was the development of knee JMS's. In 2005, Maletsky and Hillberry [37] developed a knee JMS with full displacement and force control. Up until the design of this simulator, most knee simulators applied forces at frequencies that were appropriate for simulating walking or stair climbing. Maletsky's goal was to develop a simulator that was capable of applying forces at frequencies on the level of athletic activities. Motivating the study was the implantation of prostheses in younger and younger patients. The system represented a lower extremity from the hip down. The hip was able to translate vertically on a sled and rotate about a pin joint connected to the sled. A linear actuator attached to the femur provided a quadriceps force. Three more degrees of freedom were provided by a ball joint at the ankle. This JMS was another example of a slider crank style knee JMS, by far the most popular. There were four goals in the development of this simulator which showed its wide ranging use: evaluation of an extensive dynamic model that was developed, evaluation of the ankle flexion moment's effect on knee loading, measurement of forces on the knee during simulated walking,

and examination of cross coupling between the knee flexion angle and the other axes. Control of the system primarily involved displacement control of the quadriceps with the remaining muscles under load control. The controller was designed and implemented in LabVIEW and ran at approximately 5 Hz, which at first seems to be slow, but when considering the speed of other simulators, this was actually very fast.

JMS's in some form have been used for over 50 years. Their progression has been driven by the need to actuate cadaveric specimens in physiologic conditions, to elucidate the effects of prostheses, and provide new insights into the mechanics of joints. Computer control has greatly increased the flexibility in testing parameters and repeatability. It is for these reasons that it is critical to build a computer controlled JMS to produce the most clinically relevant data.

3.0 METHODS

A number of steps were required to develop a multi-axis closed loop feedback system. The control hardware had already been purchased. The problem was to create the desired system with what was at hand. The following sections describe the hardware that was used to actuate, monitor, and protect an elbow joint motion simulator and the software that was used to control that hardware.

3.1 FEEDBACK REALIZATION WITH AVAILABLE HARDWARE

3.1.1 Elbow Frame

Support for the elbow, motors, and pulley system for the application of loads was provided by a specially designed frame. The design of this frame was detailed by Magnusen in [38]. Kuxhaus et al. [39,40] validated the applied moment arms by comparing values measured with those reported in the literature.

3.1.2 Controller and Breakout Box

The Parker Hannifin system used to actuate the elbow is comprised of a number of parts. The first part is the controller itself, an ACR 8020 8-Axis controller. The controller interprets the code written in ACRView, reads analog and digital inputs, and produces the necessary outputs to command the drives.

The controller itself is a card within a computer making direct input and output connections impractical. Instead a breakout box, RBC 8408, is connected through four ribbon cables to the controller. It is the breakout box which provides physical access to the controller's inputs and outputs. Digital inputs provide means for connecting limit switches which will be discussed later. The eight available analog inputs provide means for reading position data from potentiometers or inclinometers and force data from load cells. The breakout box also provides the physical connection between the drives and the controller; it is the physical extension of the controller's input / output.

3.1.3 Actuators

Although the controller performs the calculations to produce the necessary motions to move the arm appropriately, it lacks sufficient power output to drive the motors. This is the job of the drives. The drives, Gemini GV Series, take the motion commands the controller produces and provide the power to move the motors appropriately. They are analogous to large transistors; a small signal from the controller commands a much larger one. This analog voltage method is called the 'servo mode' within the framework of the controller. The system can also be driven with pulse width modulation which is deemed the 'stepper mode'.

The motors, BE series, are rotational servo motors with built-in encoders which feedback motor position and velocity data. Linear motion is produced by connecting ballscrew actuators to the motors. The feedback signals are not that useful for those actuators in which the ballscrews are connected to the arm through springs because a direct kinematic relationship does not exist. In an ideal situation, if initial conditions were taken and a dynamic model was known, this encoder data could be used for control instead of the sensors connected directly to the arm measuring joint angle. This model would introduce unnecessary error into control since the displacement measurement of the arm position currently used is not difficult.

The motors are capable of two sorts of movement: moves of predefined length with the “move” command and moves of indefinite length with the “jog” command. The former is commanded with two inputs: axis and distance. The motor moves this distance based on predefined settings of acceleration and velocity. These values cannot be changed during movement. In terms of doing feedback control, the “move” command is not useful. The “jog” command however provides a route through which a discrete feedback loop can be realized.

Each axis has individual, controllable bits for jogging forward and jogging backward. Only one directional bit can be set at a time; if the user tries to set them both, the more recent one set will stay on and the previous one will be turned off. Each axis also has a parameter controlling the jog velocity. To clarify, bits are values that are on or off, whereas parameters have a single-float or long-float value. Fortunately, this velocity parameter value can be changed while the jog bit is set and the motor is in motion.

Ideally, the transition from a positive velocity input to a negative velocity and visa versa would be seamless and the controller velocity parameter could handle a positive or negative

value. Unfortunately this is not the case and logic must be used to set the appropriate direction flags and set the velocity parameter to a positive semi-definite value based on the control signal.

The logic for this is as follows. A PID control algorithm outputs a value which is proportional to the desired velocity of a given actuator. This value can be positive, negative, or zero. If the value is positive, the jog forward bit is set and the given axis jog velocity parameter is set to the value of the controller output. If the value is negative, the jog backward bit is set and the given axis jog velocity parameter is set to the absolute value of the controller output. If the value is zero, the given axis jog velocity parameter is set to zero and in the interest of saving code length, the current direction is unchanged.

Through this method it is possible to enable the typical servo feedback loop for either force or displacement. It is also important to note that if PID control is used to speed up the response of the system, the control signal, not the error signal, must be used to determine the direction of motion. It is possible for the input and the output signals of a PID controller to have a different sign.

On a final note, in certain instances based on the choice of actuator, a certain sign for the control output will not always imply the same direction of actuator movement. For example, if the triceps actuator performs displacement control and the control signal is positive, it implies that the arm needs to be flexed corresponding to triceps extension. On the other hand, if the triceps actuator performs force control and the control signal is positive it implies that the force in the triceps cable must increase corresponding to triceps retraction.

3.1.4 Sensors

One of the key goals of the elbow joint motion simulator is to be able to move the arm through desired trajectories under chosen loads. Before controlling the load, it has to first be measured. Load cells are sensors capable of measuring force. Load cells can be bought for force measurement in tension, compression, or both. They can also provide measurement for single or multiple axes. There are also different architectures for load cells which provide certain limitations to their use. The most common design for a load cell is the strain gage load cell, where resistive elements are connected to an elastic member. As a load is applied, the elastic member is deformed, changing the resistance of the transducers thereby changing the output voltage. This output voltage is measurable, providing a scaled measurement of the load. Strain gage load cells provide the desirable characteristic of DC load measurement and were thus chosen.

Within the scope of this project, it is only necessary to measure the tension in the cables that connect the linear ballscrew positioners to the arm itself. Putting a single axis load cell in series between these two elements provides the desired measurement as the tension is constant through a series connection.

It is also important to choose the appropriate size load cell. The noise and accuracy of a load cell is a function of its full scale load. Therefore it is important to consider the magnitude of the applied loads before buying a load cell. That way, the smallest load cell can be chosen that provides the least amount of noise, but an acceptable upper load limit that won't be crossed. Most load cells have a maximum applied force of about 150% of full scale before they are permanently damaged.

With consideration of the simulator's performance requirements a maximum load of 25 pounds for the biceps brachii and pronator teres, and 50 pounds for the brachialis and triceps were deemed reasonable. Load cells from Transducer Techniques were chosen based on their performance characteristics. The MDB Ultra Precision Mini Load cells were chosen in 25 and 50 pound models.

The output of the load cells is routed to Daytronic Model 3170 strain gage conditioners. These conditioners provide controllable gain and offset so the desired input can be tailored. Because of the functionality of the ACRView software, load cell calibration is typically performed within the controller.

The control of displacement also requires a means to track both the F/E angle and the P/S angle. For P/S, a potentiometer is connected to a mechanism that is rigidly attached to the ulna with a pivoting arm that connects to the radius. The axis of the potentiometer and the portion of the mechanism connected to the ulna do not move relative to one another. The body of the potentiometer rotates with the arm of the mechanism and the radius. In this way the output of the potentiometer varies with P/S angle. A Novotechnik P1401a potentiometer is used. The potentiometers are powered by a 5V signal from a Hewlett Packard HP6284A power supply. Figure 2 illustrates the arrangement of the required hardware for P/S control.

The F/E angle is fed back by means of a X3Q inclinometer from US Digital. This is a device that uses MEMS technology to output a quadrature signal. A quadrature signal is composed of a pair of square waves that are 90° out of phase. The lead or lag of this phase indicates the direction the inclinometer is being rotated and the frequency of the square waves indicates the speed at which it is being rotated. US Digital also manufactures the EDAC2 converter which takes the quadrature output of the inclinometer and outputs a voltage

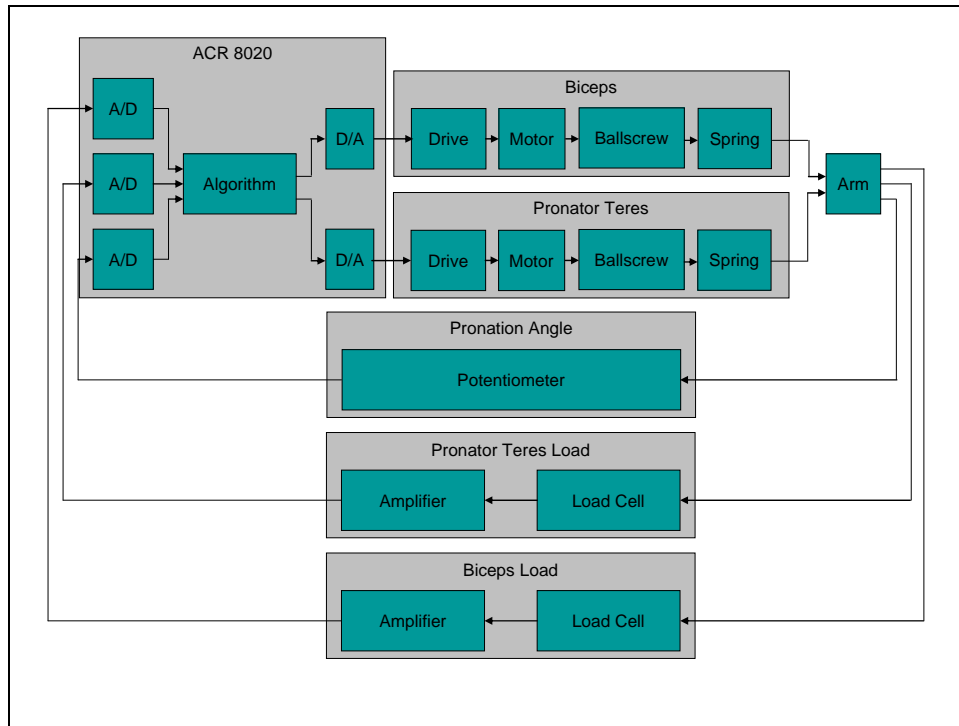


Figure 2. Illustration of the hardware arrangement to perform P/S

proportional to the angle of the inclinometer's body. Figure 3 illustrates the arrangement of required hardware for the F/E control.

3.1.5 Sensors for System Protection

During the testing of new control algorithms it is paramount to have some sort of safety mechanism to prevent damage to the motors, ballscrew positioners, or arm in the event of instability. The system must contain not only a sensor to indicate the end of travel, but some sort of software with a high sampling rate to read the sensor and quickly stop the system. The sensor is a limit switch which is a basic Hall Effect sensor designed by Parker Hannifin to be directly integrated into the system specifically for this purpose. The software comes in the form of a

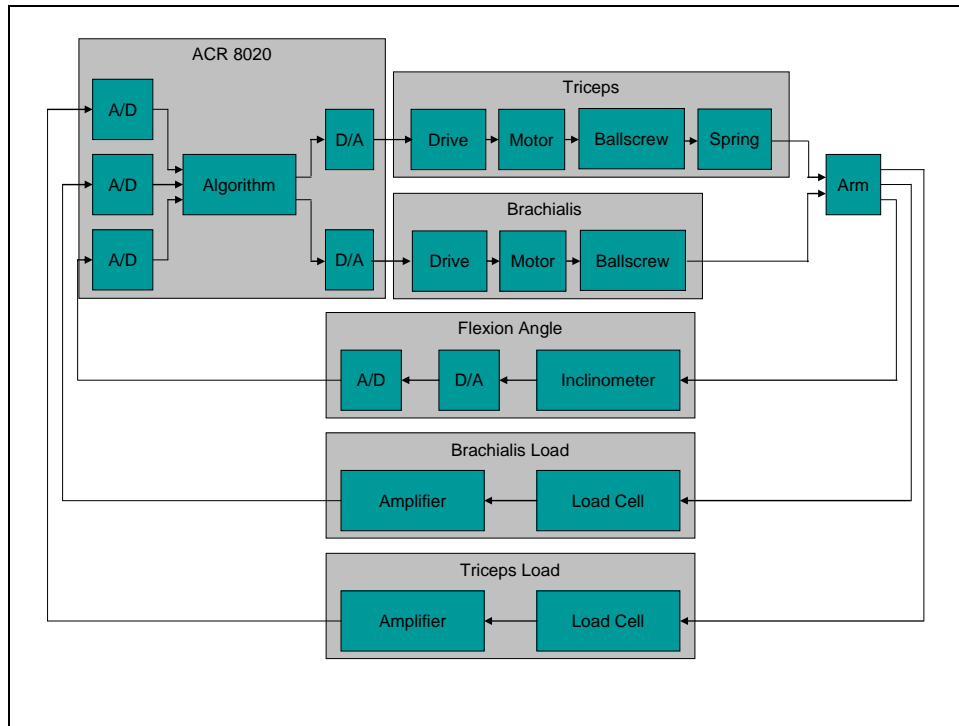


Figure 3. Illustration of the hardware arrangement to perform F/E

programmable logic controller (PLC) used to link the state of the sensor with the control bits permitting movement that will be discussed in a later section.

In a Hall Effect device, charge flows across a structure such as a plate, where it is evenly distributed; perpendicular to the direction of flow there is no potential difference. In the presence of a magnetic field, the charge is pushed in the direction orthogonal to the current flow and the magnetic field, creating a potential difference across the plate [41]. This effect can be used to create a travel limit sensor by providing a current carrying plate affixed to the stationary positioner housing and a magnet affixed to the moving ballscrew positioner. When the plate and magnet are inline, a voltage is measurable. This voltage can then be used to open a switch indicating that the end of travel has been reached. By placing two sensors on each positioner housing both full extension and full retraction can be prevented. Figure 4 illustrates the three

cases that can occur with the limit switches. Note that the sensor level goes low only at the limit, motivating the following discussion of the latch assembly.

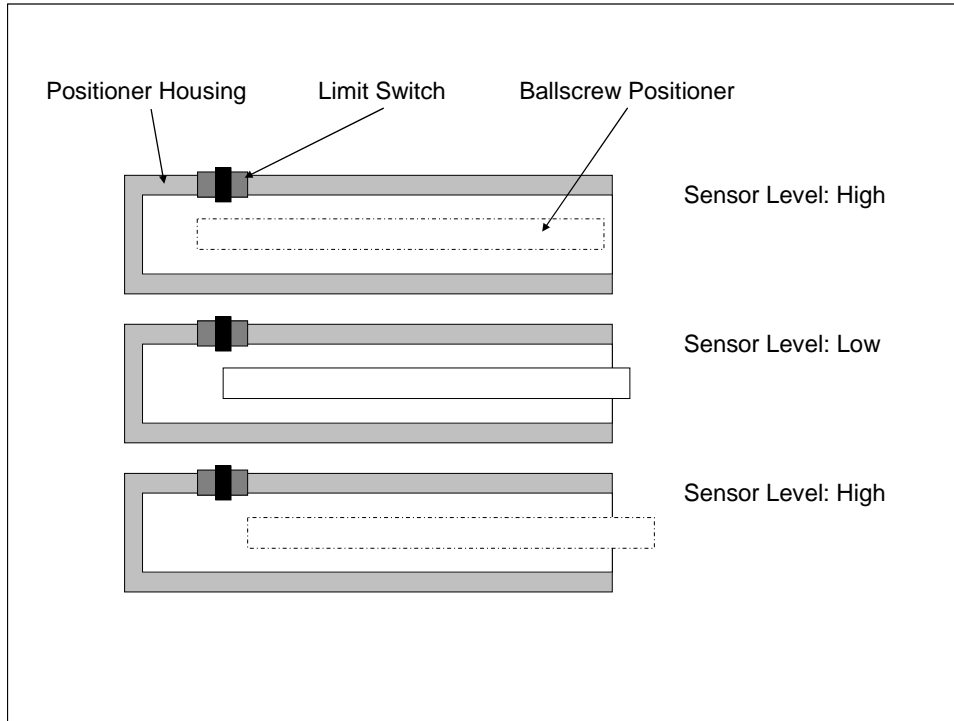


Figure 4. Limit switch output relative to ballscrew position

3.2 PID CONTROL

3.2.1 Discrete PID Algorithm

To accelerate response and alleviate steady state error, PID controllers have been added to all of the servo control loops.

The standard Laplace domain transfer function of a PID controller is as follows.

$$\frac{u(s)}{e(s)} = K_P \left(1 + \frac{1}{T_I s} + T_D s \right)$$

This transfer function can not be digitally implemented and must be discretized.

Returning to the time domain will yield the following continuous relationship:

$$\dot{u}(t) = K_P \dot{e}(t) + \frac{K_P e(t)}{T_I} + K_P T_D \ddot{e}(t)$$

The following backward difference can discretize the continuous derivative terms. The transfer function is temporal so the backward difference is chosen to keep the system causal.

$$\dot{x}(t) \approx \frac{x(k) - x(k-1)}{T}$$

This substitution will yield the following digitally implementable PID controller, the constants have been combined so that there is one constant per term.

$$u(k) = u(k-1) + [K_P + K_I + K_D] e(k) - [K_P + K_D] e(k-1) + K_D e(k-2)$$

A more complete derivation of the discrete velocity from of a PID controller can be found in [42].

3.3 SOFTWARE IMPLEMENTATION

3.3.1 Control Requirements

The design of this controller was facilitated by the desire to perform two separate tests: flexing and extending the arm while holding the P/S angle constant and the converse, pronating and supinating the arm while holding the F/E angle constant. Two steps were taken on the way to developing a single controller capable of doing both tests.

3.3.2 Flexion / Extension Controller

The first control design was chosen based on a desire to show that the system could in fact operate under closed loop feedback control, a critical step considering the future plans of the system. Control of the F/E angle through actuation of the brachialis and triceps was the simplest, most relevant test that would show if the system would be sufficient. Both of these muscles insert on the ulna which eliminates any complexity derived from the second degree of freedom about the P/S axis. Figure 5 shows a simple schematic of how these two muscles actuate the arm.

Acceptable stability was defined to be the ability to move the chosen degree of freedom through a chosen trajectory with adequate stiffness from small moments in either direction about a chosen degree of freedom. This second condition became very important when considering the uni-directional cable actuation which provides stiffness in opposition to a moment in only one direction, the direction in which tension in the cable increases, that is you cannot push with a rope.

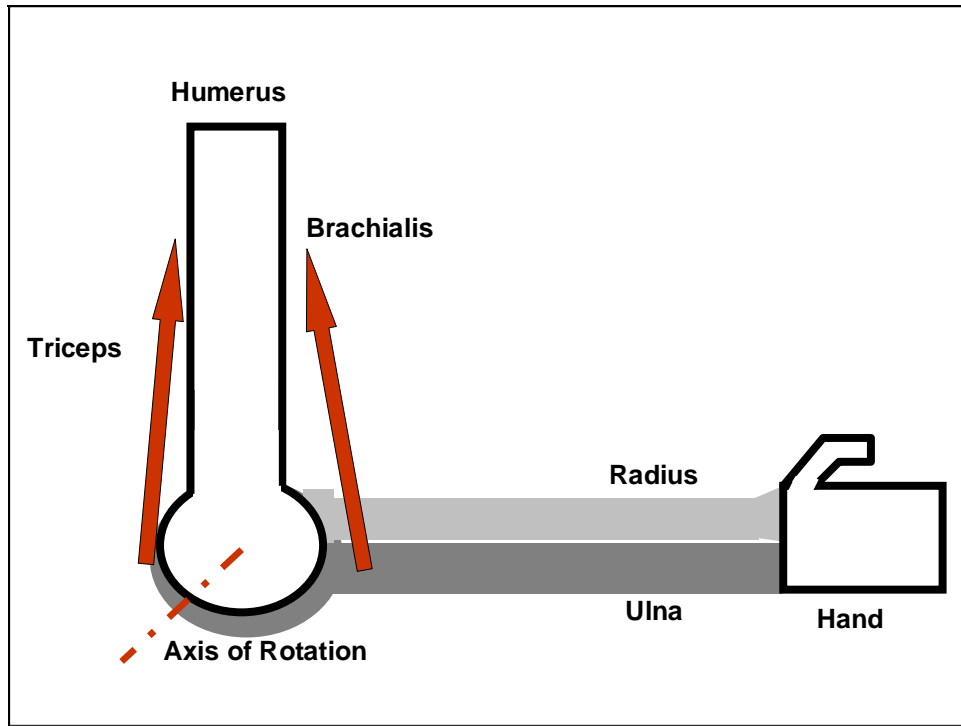


Figure 5. Muscles used for F/E controller

The approach used for the first controller was similar to that used by Dunning et al. at the University of Western Ontario in which one actuator operated under displacement control and the other actuator operated under load control. This agonist / antagonist pair provided the ability to move the joint as desired through displacement control and provided joint impedance through load control. However, this system was not completely stable in terms of the requirements listed above. In terms of motion without any sort of physical perturbation, the system worked as desired.

A simple example illustrates the instability in the face of a perturbation. If the reference angle of the arm was set at a given point and the arm was displaced above this reference angle, the motor controlling the brachialis provided slack in an effort to extend the arm. While this occurred, the motor controlling the triceps was set to maintain a given load, if this load was not

enough to overcome the load preventing the attainment of the correct displacement, the motor controlling the brachialis continued to move forward introducing slack in the cable connected to the brachialis insertion. This slack broke the stability goal listed above. It was important to consider perturbations to the F/E motion not because of unforeseen objects within the configuration space of the arm, but because the biceps and the pronator teres supplied varying flexion moments while they supinate and pronate the arm and these are treated as perturbations to F/E.

Logic statements within the code were used to fix this instability. The system functioned as listed above as long as the load in the brachialis, which was constantly being fed back, was above a user defined minimum level. If the system dropped below this point, the load and displacement control switched which muscles they controlled. In a sense, the system went from lowering the arm with brachialis, to pulling the arm down with the triceps. While this happened, stability was added to the arm by using the muscle not controlling motion to act as an antagonist, pulling at a set load in opposition to the direction of the movement. This system provided a definite improvement over the first, but was not without fault. No immovable impediment could be placed in the way of the arm. This would have led to continually increasing the triceps or brachialis loads either breaking a cable, a section of the arm, or overheating a motor. In an ideal case, in which the motors had infinite power and the hardware would never break, this system would have been stable in terms of the above conditions.

Figure 6 provides a Simulink block diagram for this control methodology. In this diagram, the switch's position is based on whether or not the measured brachialis load is greater than the chosen minimum load. If the brachialis load is above the minimum level, the top case is used and the triceps actuator is driven to maintain a certain load and the brachialis actuator is

driven to maintain a certain F/E angle. If the brachialis load is not above the minimum level, the bottom case is used and the triceps actuator is driven to maintain a given F/E angle and the brachialis is driven to maintain the minimum load.

Figure 7 provides a flow chart to better illustrate the switching logic between load and displacement control for the brachialis and triceps. The lower part of the flow chart shows that the addition of a PID controller changes the direction decision variable to the sign of the control signal which implies either the need for flexion or extension. Without the PID controller this decision is based on the sign of the error signal.

Code for the F/E controller is provided in Appendix 1, Section 1.

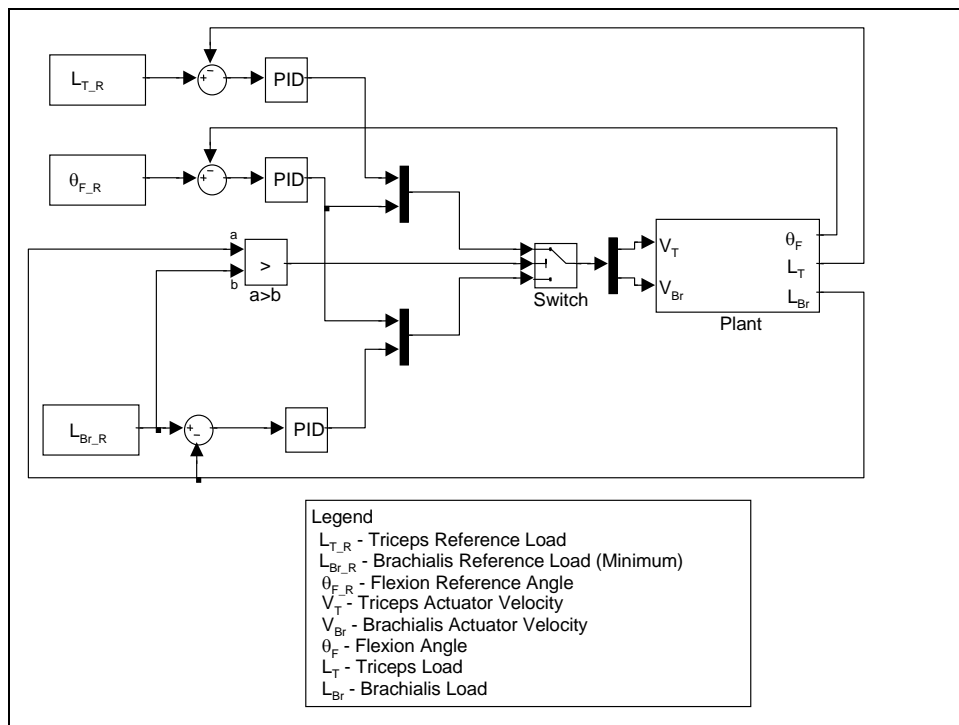


Figure 6. Block diagram for F/E controller

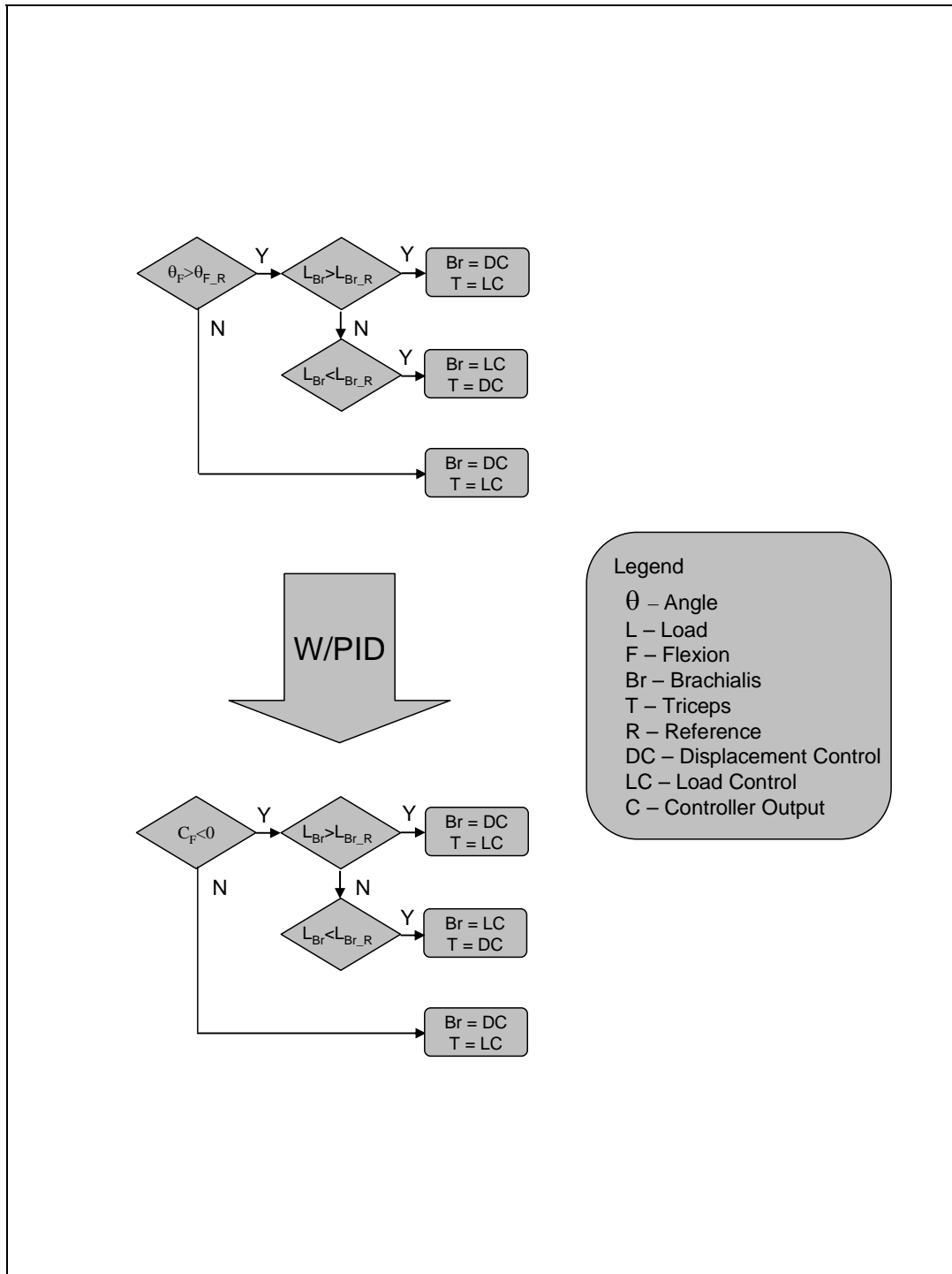


Figure 7. Determining load and displacement control in the F/E controller

3.3.3 Evolution of the Full Controller Design

Extending the controller design from the previous section to yield a controller capable of performing P/S at a constant F/E angle and F/E at a constant P/S angle was the final goal of the project. The most critical design obstacle was formulating P/S control which would be compliant to F/E motions. The control of the biceps and pronator teres needed to take up slack in flexion and provide slack in extension while maintaining the appropriate P/S angle.

The simplest idea was to mimic the method used for F/E control: one actuator under load control and the other under displacement control, with the displacement control based on maintaining the P/S angle. This method worked well for constant F/E movements. Unfortunately the actuator under displacement control could not provide or take up slack during F/E as its movement was based solely on P/S angle. Therefore, it could not provide a means for achieving the two desired motions.

The next idea was to use various bits of logic to provide a displacement control deadzone around the correct P/S angle so that within that deadzone, the previously displacement controlled actuator could be load controlled making it compliant to F/E. This system showed some success, but had two shortcomings. First, changes in force when the system crossed the deadzone boundary were generally sudden and caused jerking movements. In a system with agonist / antagonist pairing, jerking movements easily led to oscillations because of the sequential nature of the code. As each actuator responded slightly out of phase to the other, a downward spiral of stability was created. Second, the use of the deadzone itself meant a certain amount of error equal to the width of the deadzone was immediately accepted into the system. Details of this system are provided in [43].

The development of this system was important however because it led to an important realization: both the biceps and pronator teres must both be under load control if they are going to be compliant to F/E. Figure 8 provides a simple illustration of how the two muscles apply loads to the radius and ulna creating P/S motion.

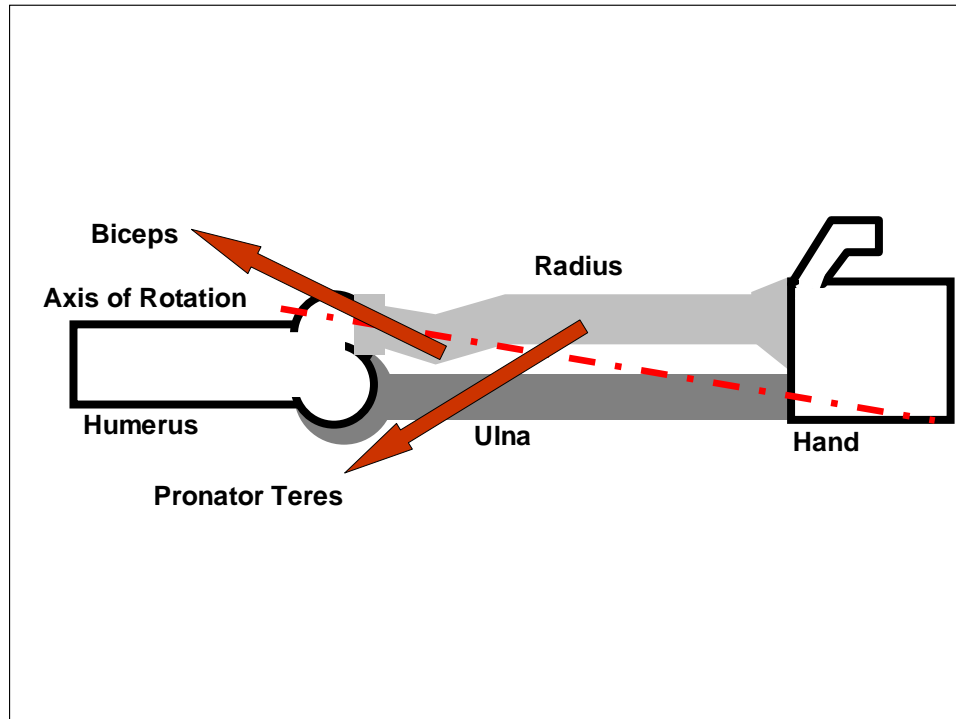


Figure 8. Muscles used for P/S control

In the late 1980's, Jacobsen et al. [44] reported a system used on a mechanical hand in which the position error was modified and added to a minimum desired load to create a signal that an actuator would interpret as a loading command. Their system also negatively fed back velocity adding damping to the system. This design formed the basis for the control method of P/S in this thesis.

The design of this controller was made in two different steps. The first step, mentioned previously, was to determine that both actuators should be force controlled. This meant that a load control servo loop, augmented with a PID controller, would be used to generate a control signal which would command the actuator's velocity to maintain some reference force.

The next step was to build an algorithm to determine the reference force. Similar to Jacobsen's design, a minimum force level was required because the cable could not be compressed. The reference force must be positive definite to prevent slack. Added to the minimum force, a positive semi-definite value related to displacement error, created the necessary net moment to rotate the radius. The displacement error could be positive, negative, or zero so it had to be modified and diverted appropriately to augment the loads correctly. Jacobsen et al. solved this problem using half-wave rectifiers which diverted the positive values to one actuator and the absolute value of negative values to the other actuator. A logical switch within the controller's program achieved the same effect. If a displacement control servo loop were to be used, again augmented with a PID controller, a positive output signal would imply a need for pronation and a negative signal would imply a need for supination. This signal could be broken up and added on to one of the minimum tendon loads to generate the reference load for each actuator's load control servo loop. In physical terms, the switch would augment the minimum pronator teres reference load with a positive displacement control signal creating pronation and would augment the minimum biceps reference load with the absolute value of a negative displacement control signal creating supination. In this way, both actuators would have at least the minimum desired load on them in addition to any extra load required to attain the desired displacement.

Figure 9 illustrates the decomposition of a sine wave by the switch into negative and positive portions. In the case of the described controller, the value decomposed is the output of a PID controller whose input is the displacement error. Figure 10 provides a Simulink block diagram of the P/S controller containing the switch. In the figure, the first summing junction creates an error signal based on measured position and desired position. The next summing junction adds the minimum load to the displacement control signal creating a reference load for the final stage. The final summing junction creates the control signal actually sent to the motor to attain the desired load.

Code for the final controller can be found in Appendix 1, Section 2.

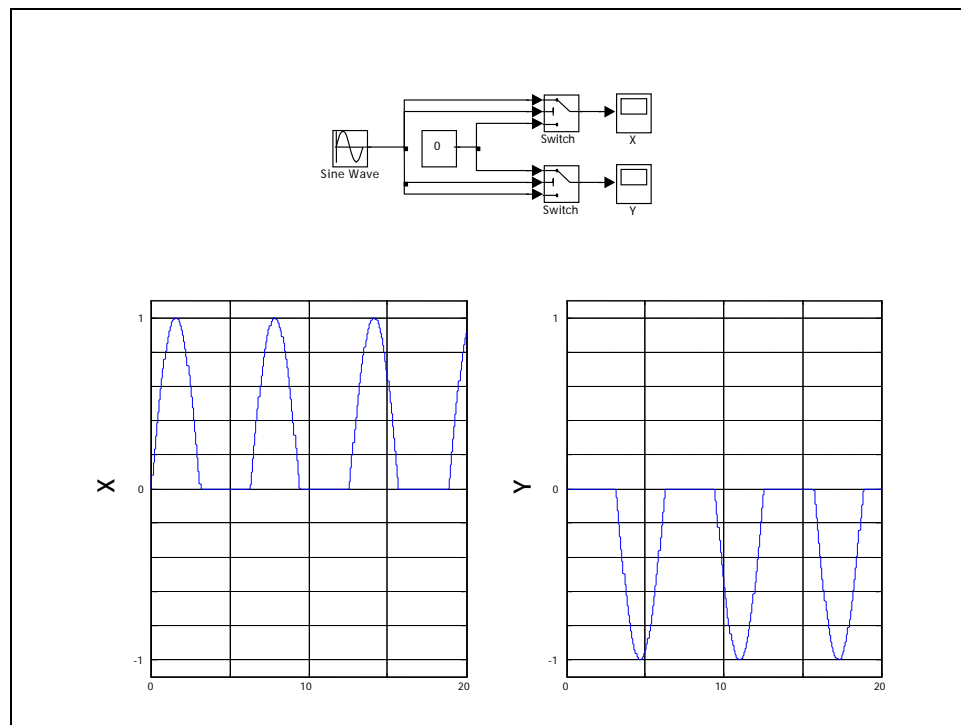


Figure 9. Effect of switch on a sine wave

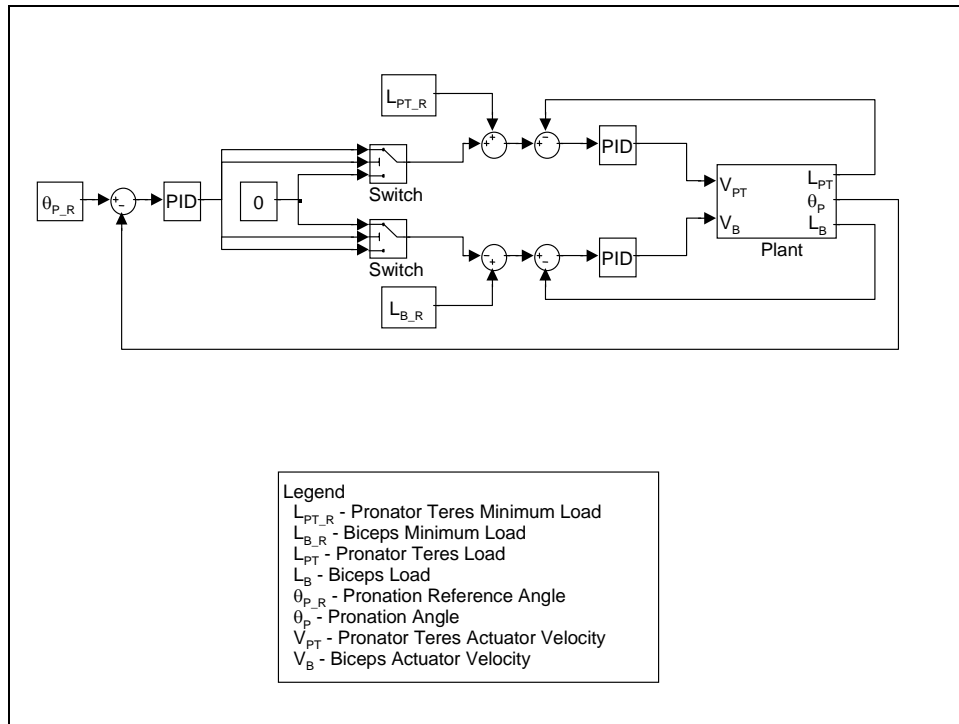


Figure 10. Block diagram of P/S controller

3.3.4 Programmable Logic Controller for Limit Switches

The programmable logic controller (PLC) within the ACRView software checks limit switch status and decides whether or not the system is still within its allowable region of travel.

Originally, PLC's were invented to replace large control systems used in automated manufacturing. Large arrays of wires and relays provided many opportunities for design mistakes, wiring mistakes, and failure of mechanical parts. General Motor's Hydromatic Division was the first to create a PLC in 1968 that is in the form used today [45]. This new electronic system replaced all the mechanical parts with a computer program enabling simpler trouble shooting and updating.

The computer programs controlling PLC's are typically written in code known as ladder logic. It is called this because the whole program is a list of circuits known as 'rungs.' These

rungs represent the flow of power from left to right. These rungs provide power to ‘coils’ along the right edge of the rung. There can be numerous coils per rung. These are the outputs of the PLC. The most basic element which can precede a coil is a contact. This is basically a relay with two states. Contacts come in two varieties: normally open, illustrated by two separate vertical lines, and normally closed, illustrated by two vertical lines connected by a diagonal line. A normally open contact provides a closed circuit when the bit it represents is high whereas a normally closed contact provides a closed circuit when the bit it represents is low.

The arrangement of contacts determines the logic of simple PLC programs. Figure 11 shows both “and” logic and “or” logic. With “and” logic both contacts 1 and 2 must be closed to set coil 3, but either can be closed to set the coil with “or” logic. It is important to note a coil’s status will pulse on and off with the contact. In many instances, such as our limit switch case, it is desirable to have the coil remain in a given position once the contact’s status changes. A latch, simply made out of two contacts and one coil, provides this effect and is shown in Figure 12. It should be noted that the second parallel contact and the coil are linked to the same bit intentionally; this is what creates the latch. If bit 1 pulses, the coil is set, this in turn sets the contact for bit 2. Now that contact 2 is set, it keeps the coil shut permanently.

All these features available in ACRView’s PLC structure provide a means for integrating a travel limit safety system into the elbow JMS. The eight limit switches are connected directly to the breakout box’s digital inputs 16-23. These digital inputs correspond directly to bit flags within the ACRView structure.

As previously mentioned, speed is important. The controller has a preset PLC interrupt rate of 0.5 ms. Every 0.5 ms it takes one step forward through a list of preset tasks. Each PLC that is running is an event on this list. To ensure that this speed is attainable, there is a 200 line

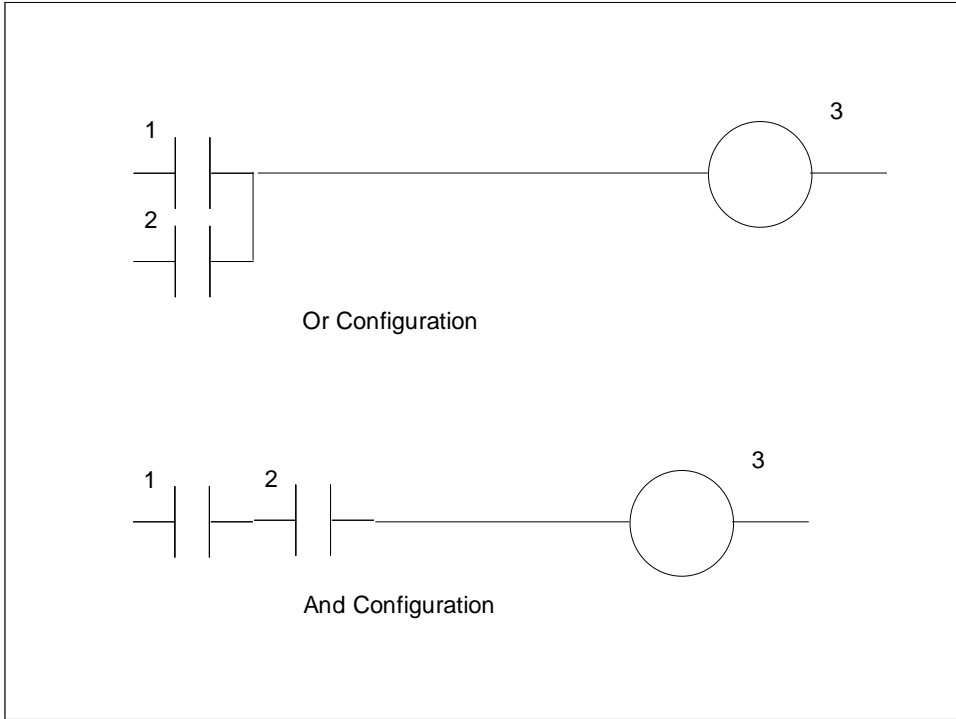


Figure 11. PLC or / and configurations

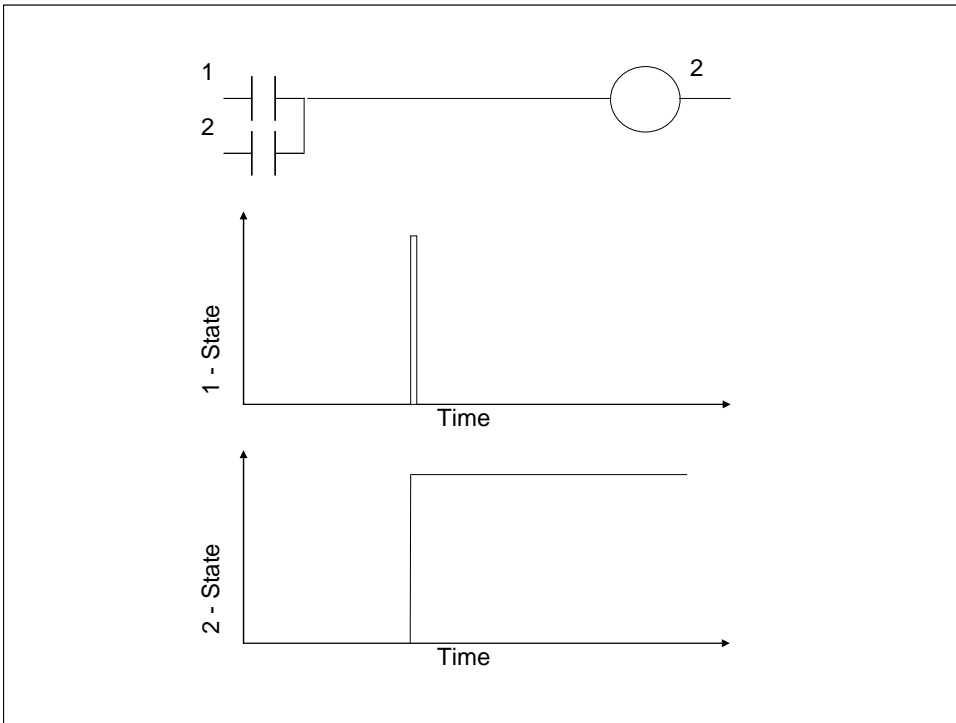


Figure 12. PLC latch signals

limit on the length of PLC programs in ACRView. In addition to the PLC's, ACRView scans the inputs and outputs and handles counters and timers. These last two tasks are not controllable, but are always present. In the current program, there is only one PLC, which means that the PLC is scanned every 1.5 ms.

Figure 13 shows a ladder diagram of the PLC used with the limit switches. Contacts 16-23 are normally closed which means they are low when closed and high when open. If any one of the limit switches goes low, bit 128, free to be used by the programmer, is set. Because bit 128 is both a contact and a coil, it acts as a latch and will stay set regardless of status of the limit switch once it is initially crossed. Bit 522, the "kill all moves" bit, is the other coil in parallel with 128. Once this bit is set, all motion due to move commands is stopped and no new move commands will be accepted until 522 is cleared. This rung is effective in stopping only moves due to move commands; it has no effect on jog commands which are used to drive the servo loops. The rungs in Figure 14 use bit 128 to stop motion due to jogs. In these rungs, a normally closed contact is used with bit 128. In effect, once bit 128 is set by a limit switch in the first rung, it opens eight previously closed circuits that allowed jog commands to be enacted.

In the event of a limit fault, the program should be halted, the PLC should be halted, the axes reset, bit 128 cleared, and bit 522 cleared. From here the system can be repositioned in an acceptable range location and the PLC and program restarted.

It should be noted that the limit switches were used to protect the motors from end of travel problems. They do not protect the arm, load cells, potentiometers, inclinometers, or any other remaining piece of hardware. As soon as an end of limit is reached, the physical system will freeze regardless of the effects of the current load conditions. To protect the load cells and arm from damaging loading conditions, the cable must be chosen so that it will break before

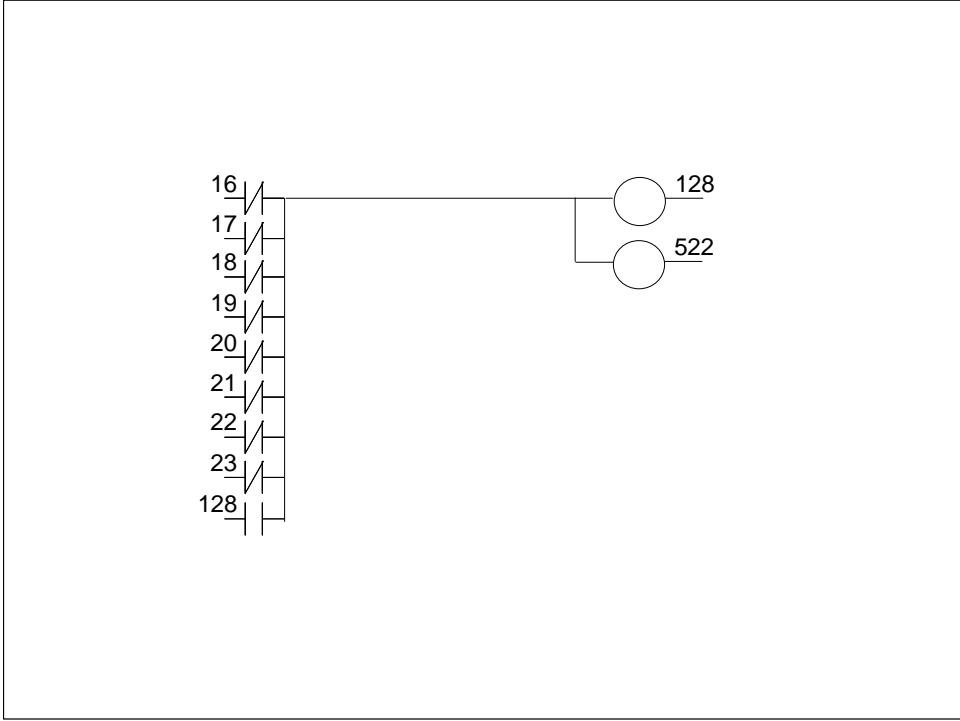


Figure 13. Move killing limit switch PLC

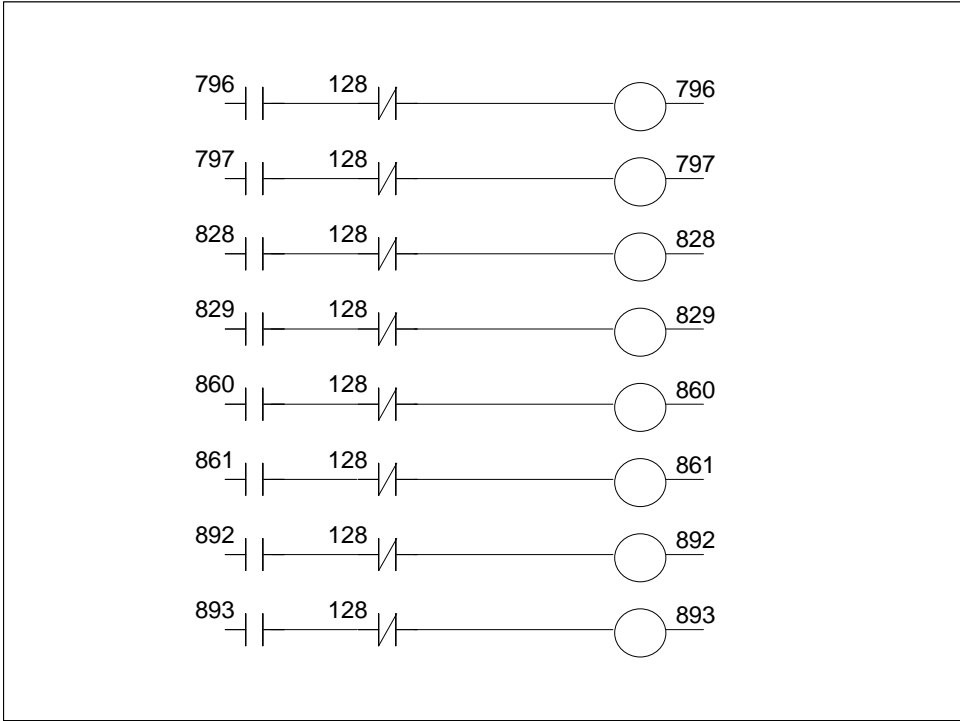


Figure 14. Jog killing limit switch PLC

harming the rest of the system. Between the load cells and the appropriate cable, the physical system should safe be from instabilities.

4.0 RESULTS AND DISCUSSION

4.1 PERFORMANCE MEASURES

The goal of the control system was to accurately and precisely actuate an elbow specimen through two types of motion: F/E with fixed P/S angle and P/S with fixed F/E angle. The system needed to be evaluated quantitatively. The accuracy of the system was first measured by determining the average error between the reference signal and the measured location. Due to lags in the system, an accuracy measurement was more meaningful if the system delay was subtracted from the measurement. It would have introduced a DC bias to the error because the system constantly lagged a certain number of degrees behind the reference. This lag was calculated to be the time at which the maximum of a cross correlation measurement between reference and actual position signals occurred.

To actually calculate the average error with lag removed, zeros were added to the beginning of the reference signal. These additional samples lined up the two signals. The number of zeros added was the same as the number of samples the actual position lagged the reference. The adjusted reference signal was then subtracted from the actual position signal and this resulting vector was then averaged. It must be noted that these signals were initially of different length due to the addition of zeros to remove lag. If N was the length of the original signals and M number of samples one signal lagged behind the other, the adjusted reference was

of length $M+N$: M zeros followed by a the original reference signal of length N . The actual position signal was still of length N . The error was calculated only with meaningful data. The initial part of the signal with the zeros and the final section of the signal, also the length of the zeros, were omitted. In terms of programming, the “for loop” started at sample $M+1$ and ended at sample N for the error calculation. Figures 15, 16, and 17 illustrate the process of calculating the lag and shifting the signals to remove the lag.

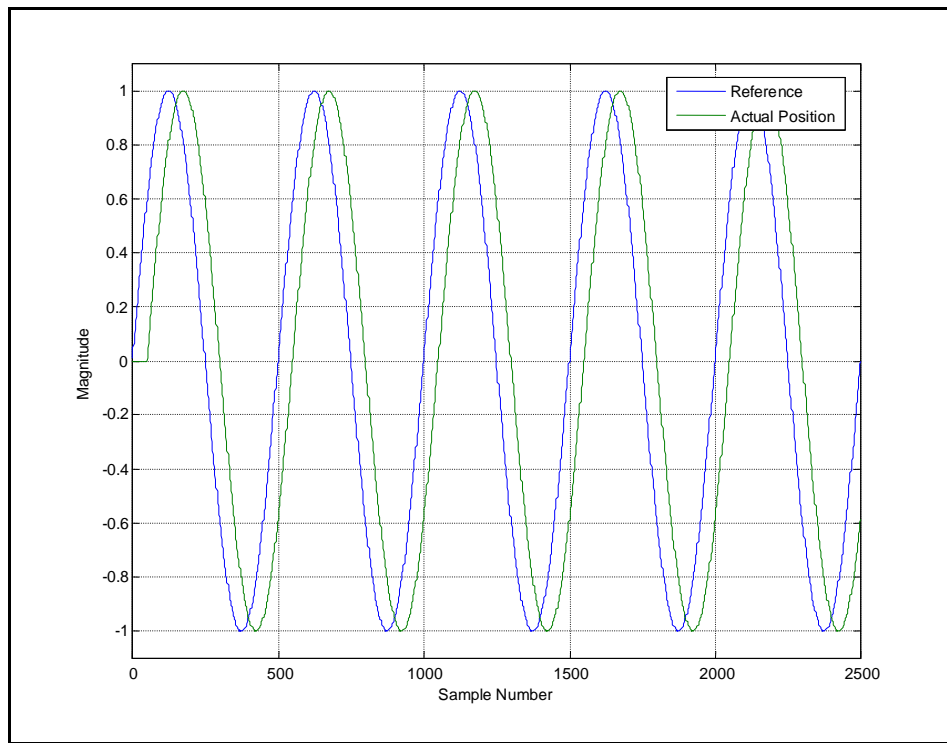


Figure 15. Two sine waves offset by a constant lag

Insight into the system was also gained by examining the standard deviation of the error signal. As will be seen, this parameter was extremely important because the mean error was extremely low in certain cases. It would have been misleading to only report this as a signal that oscillates about zero can have zero mean error regardless of its actual magnitude.

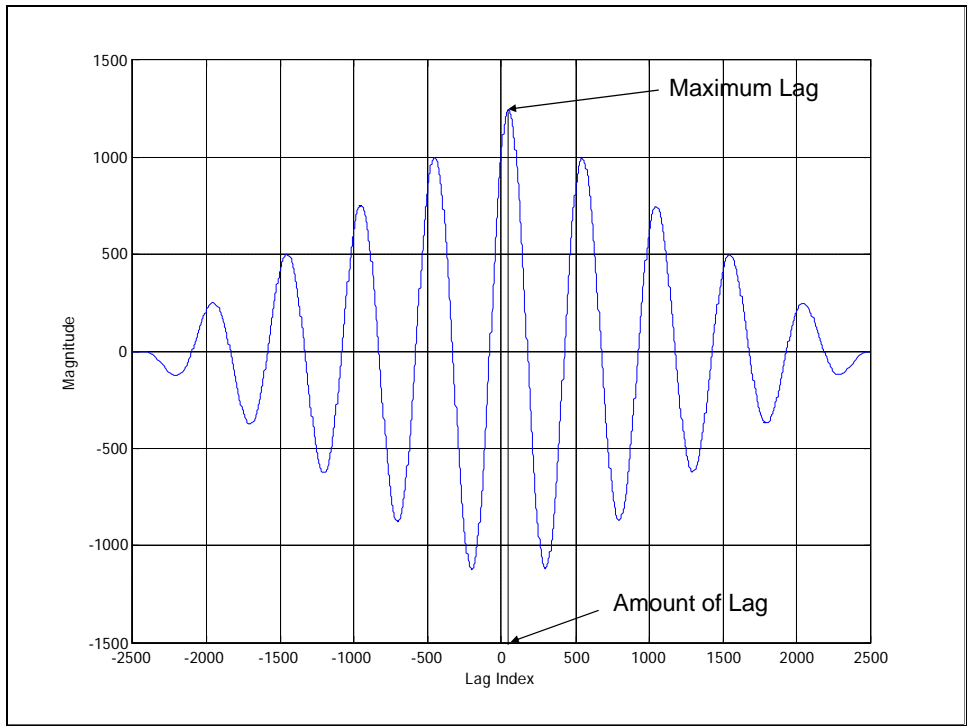


Figure 16. Cross correlation of the two sine waves

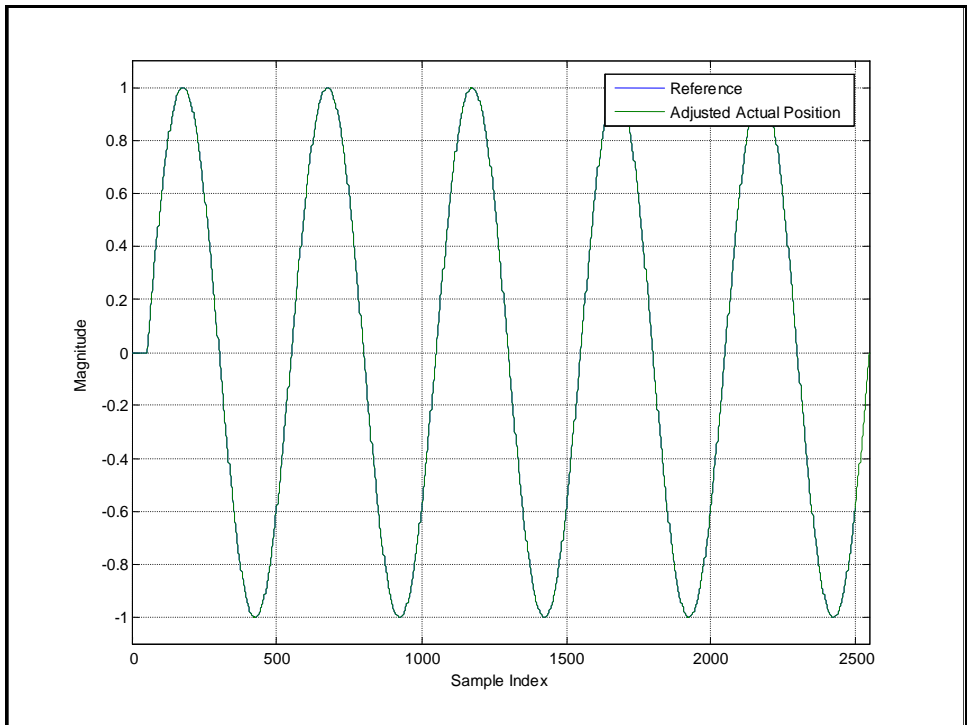


Figure 17. Successful removal of lag from two sine waves

To determine precision, three trials were taken. Then, the standard deviation as determined at each sample point between the three trials was calculated. This produced a single vector of standard deviation values as long as the trials themselves. This number was then averaged across the single vector to determine the system precision from trial to trial. It was critical to use the same reference signal for all trials; else the measure had no meaning.

The average error and average standard deviation were calculated for all controlled variables: loads and displacements. Lags and precision were calculated for signals whose references were sinusoidal. In all cases this was one displacement signal: either F/E or P/S.

It was desired to have mean error, standard deviation of error, and precision all better than 1° for the degree of freedom being maintained at a constant angle. It was also desired to keep the maximum error as low as possible.

4.2 FLEXION / EXTENSION CONTROLLER

The performance of the controller using only the brachialis and triceps to flex and extend the arm was not included in any final goal. It did however provide confidence in part of the design for the final controller as the final controller was a combination of simpler designs.

The system tracked a sine wave varying 45° above and below a horizontal position. The antagonistic loads were varied, and it was important to see if and how they affected the performance of the system. Tables 1 and 2 in Appendix 2, Section 1 show the results of varying the triceps loading. The results show no conclusive differences as far as the quality of the F/E motion or the ability to maintain a given triceps load. Figures 18 and 19 illustrate the data in

these tables, also confirming the lack of effect of load changes on any of the performance measures.

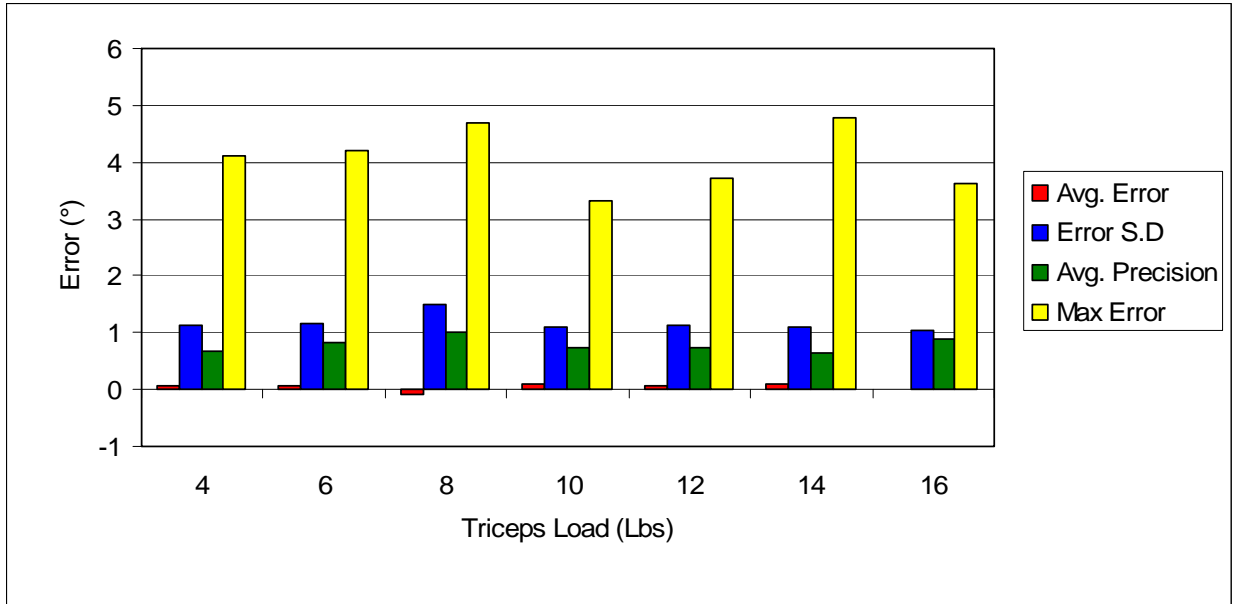


Figure 18. Maintenance of correct flexion angle during F/E tests

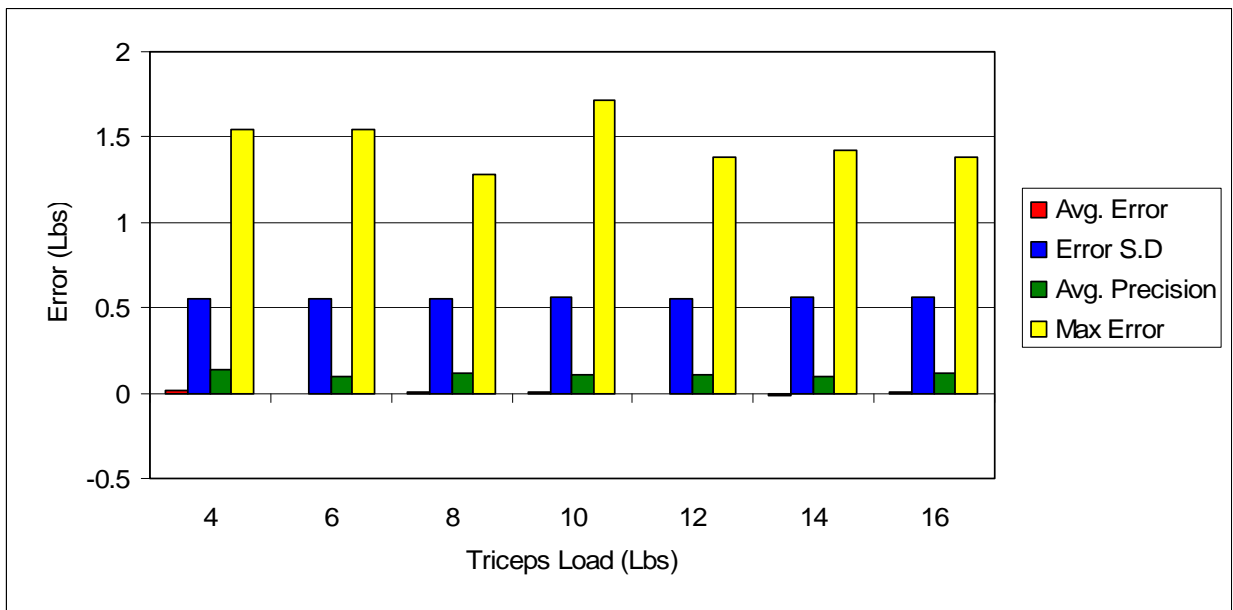


Figure 19. Maintenance of correct triceps tension during F/E tests

Figures 20, 21, and 22 provide examples of the F/E motion, the triceps loads, and the brachialis loads for the lightest loading case. Figures 23, 24, and 25 provide examples of the F/E motion, the triceps loads, and the brachialis loads for the highest loading case. The repeatability of the motions and loading during the motions is clear in all cases. In general, the load control plots are 90° out of phase with the displacement. This makes sense because the triceps controller tries to maintain the load during movement, thus it reaches maximum error during movement and alleviates that error as the system slows to change direction or comes to a stop.

The biggest difference between using light and heavy triceps loads were the resulting brachialis loads. These brachialis values were not quantified as they were not controlled; rather, they were the loads resulting from the displacement control of the brachialis. They were the loads the system needed to apply to move the arm through the desired displacement motion with the triceps acting as an antagonist. At no point during the testing did the system drop below the set minimum brachialis load of 1.5 LBS. From a practical standpoint, the large brachialis loads may be undesirable because of the greater wear on the hardware, as it appears to be the only difference in performance between the various triceps reference loads.

Triceps loads vary about the reference by about one pound. The primary interest was the displacement and since it was acceptable, the varying triceps loads, which had little impact on displacement control, were acceptable. Increasing the proportional gain of the system improved this. Figure 26 provides an example of the triceps loads over a number of trials with increasing proportional gains and shows the ability to bring the load error down with increasing gain.

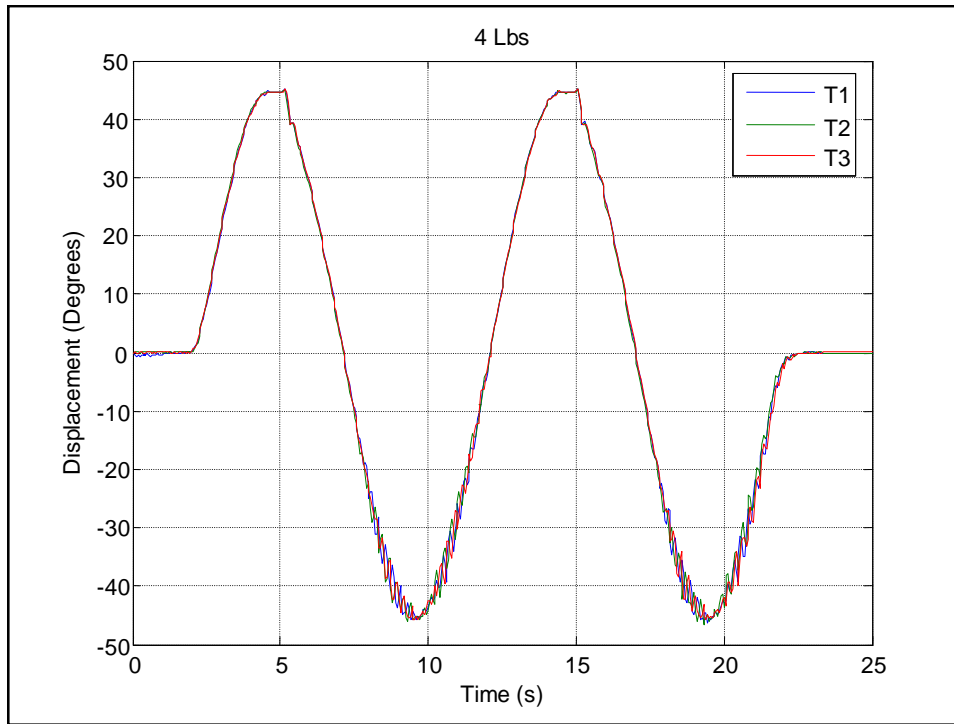


Figure 20. Plots of the three F/E trials with a triceps load of 4 LBS

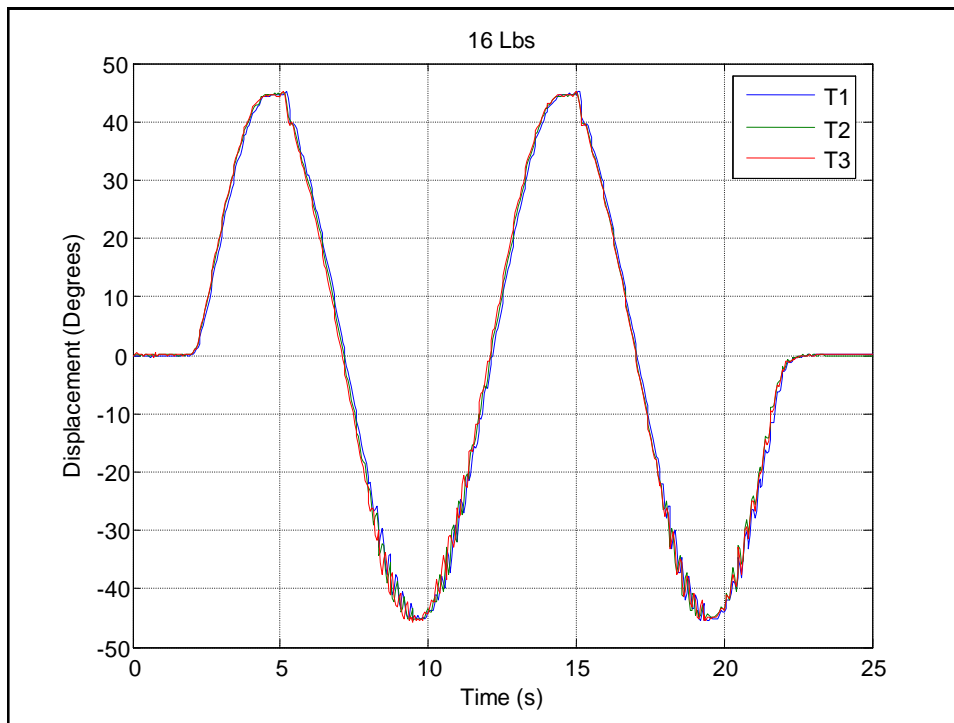


Figure 21. Plots of the three F/E trials with a triceps load of 16 LBS

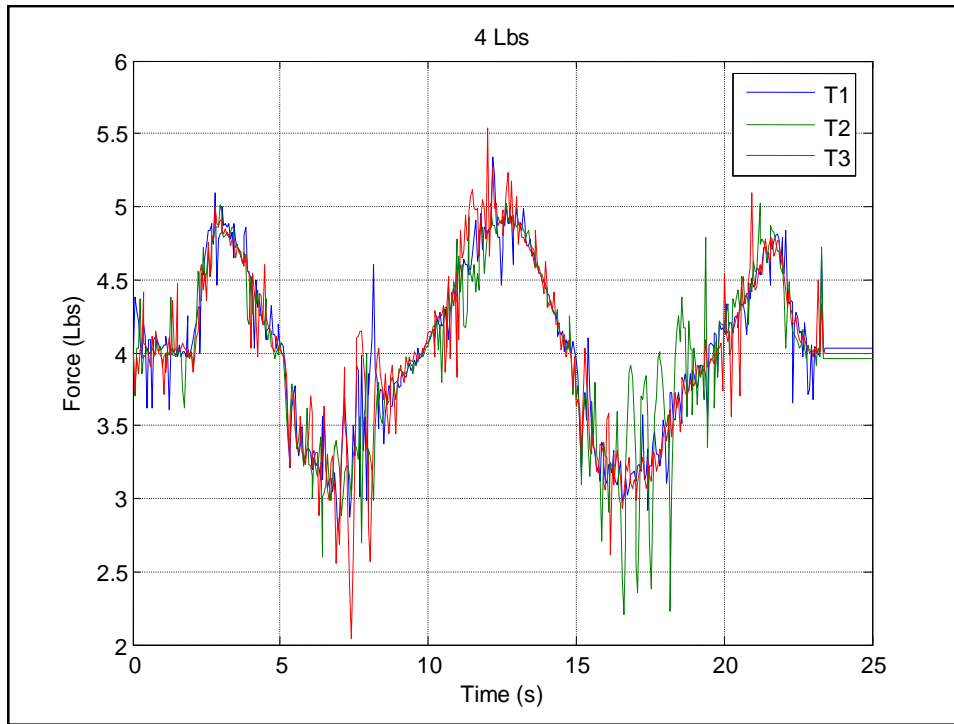


Figure 22. Plots of the triceps loads during three trials with a triceps reference load of 4 LBS

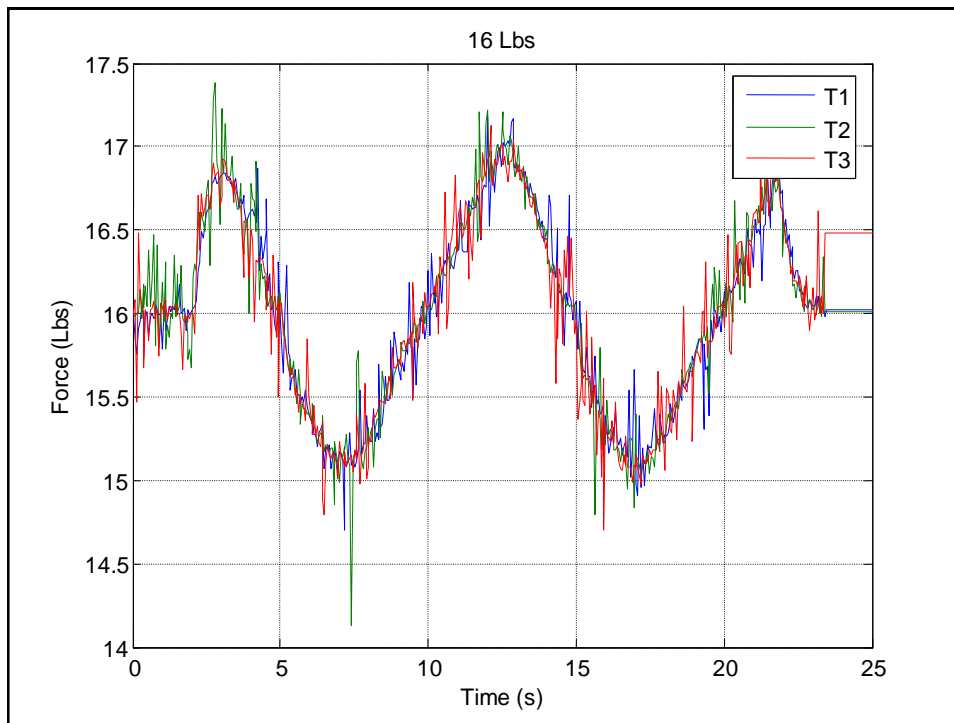


Figure 23. Plots of the triceps loads during three trials with a triceps reference load of 16 LBS

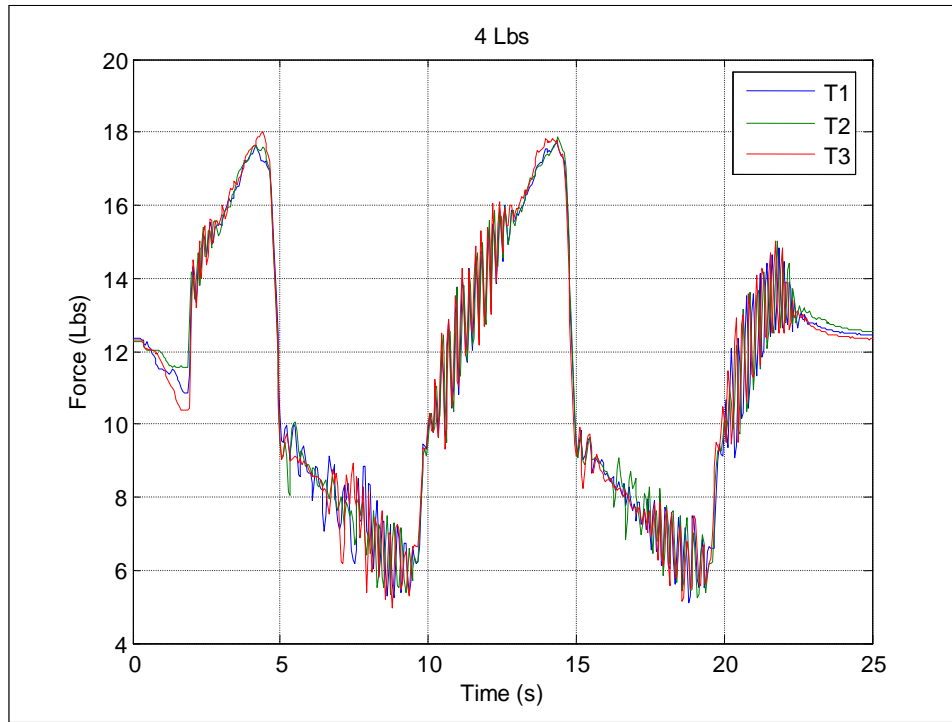


Figure 24. Plots of the brachialis loads during three trials with a triceps reference load of 4 LBS

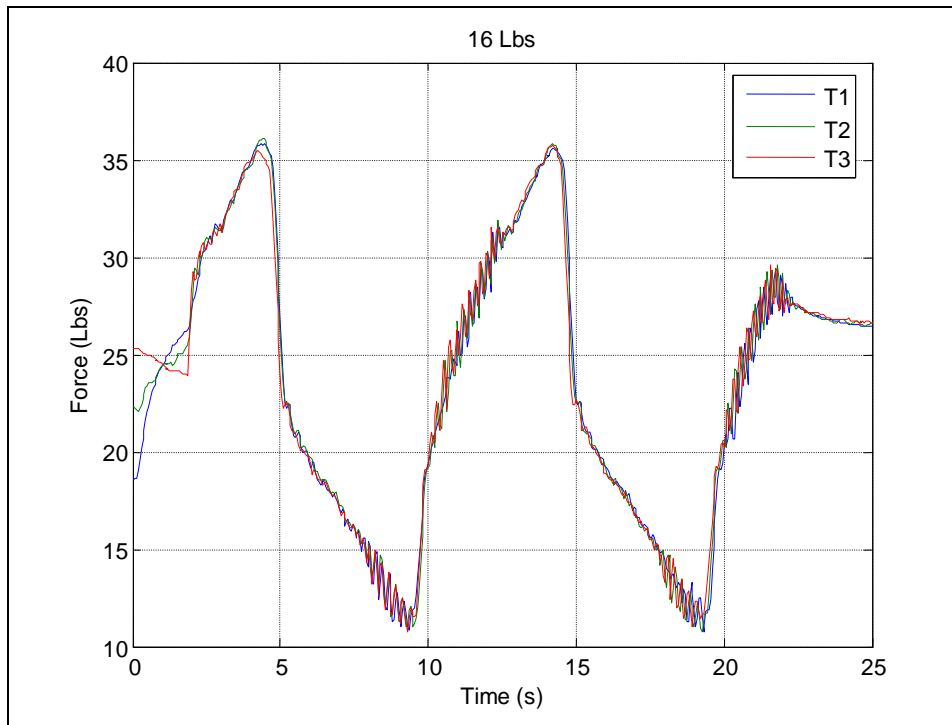


Figure 25. Plots of the brachialis loads during three trials with a triceps reference load of 16 LBS

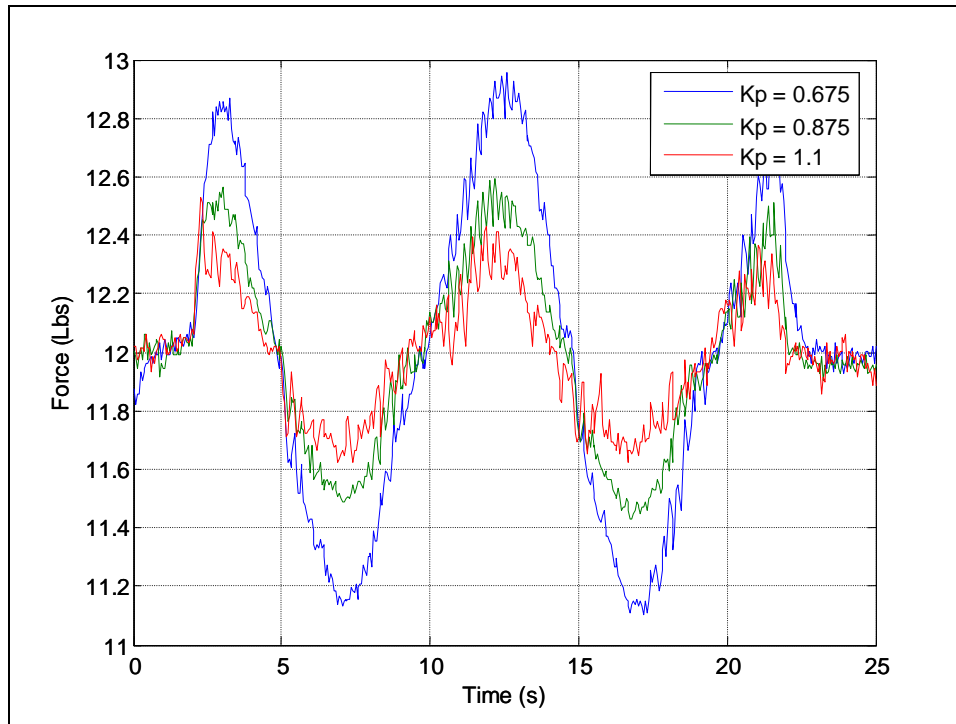


Figure 26. Improvement in triceps load control due to proportional gain increase

4.3 FINAL CONTROLLER

Before providing results of the testing of the final controller, it is first useful to describe the process used for tuning the gains of the PID controllers within the system. Three of the actuators within the system were load controlled. If the system did not reach the commanded loads, there was no utility in changing other gains which affect how those loads are determined as the true effect of these changes would be difficult to determine. So the first step is to vary the gains of the PID controllers which directly affect the load control. Once these values are satisfactory, tuning can then proceed to the gains related to the displacement control. It should also be noted that one set of gains was used for F/E and another set was used for P/S. In this way, only one variable was changed at a time so its effects could be isolated within each test.

Appendix 3 provides data tables containing all of the results of the testing. The results that provide some sort of insight or are directly related to the goals of the project are provided in the following sections.

4.3.1 F/E at Constant P/S Angle

The first test involved evaluating the system's ability to perform F/E movements at a constant P/S angle. The arm was flexed between 45° and 135° at P/S angles of -90° , -60° , -30° , 0° , and 15° . The most important part of the test was not the tracking of the F/E signal, but the maintenance of the fixed P/S angle. In addition, it was interesting to see if various triceps loads or minimum values for the biceps and pronator teres affected the ability to perform the motions.

The chart in Figure 27 shows the system is capable of maintaining the P/S angle during F/E. The mean and standard deviation of the error along with the precision are all well below a degree.

Varying the triceps load had no appreciable impact on performance, varying the minimum load for the biceps and pronator teres did however. Figure 28 shows that the precision, mean error, and standard deviation of the error all went up as the minimum load was increased. In various trials using greater loads instabilities often occurred. Control outputs are determined sequentially, not at the same time. Because of this, large loads seemed to introduce oscillations as the system was able to pull hard with one actuator, then pulled hard back, out of phase, with the other actuator, and so on. With smaller loads this effect decreased.

Figures 29 and 30 provide illustrations of the maintenance of various P/S angles during F/E and F/E motions at these various P/S angles respectively. The system was tuned at a P/S angle of -90° which may have an impact on its quality relative to the other cases. It is interesting

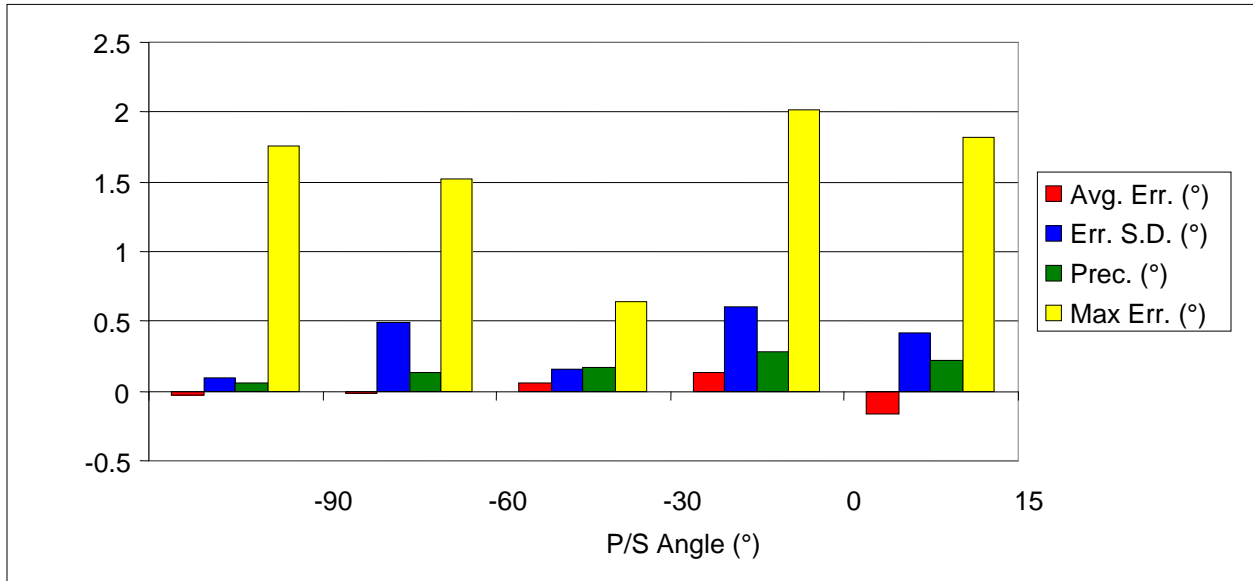


Figure 27. Maintenance of various P/S angles during F/E

to note in Figure 30, the different amounts of lag, sometimes up to approximately 2 seconds. This occurred because the controller ran at varying speeds. More will be discussed about the impacts of this later. The only difference between any of the cases was the P/S angle.

Brachialis loading during F/E trials was as expected. The brachialis was not under load control. The loads applied resulted from using the brachialis to control the F/E angle of the arm. Due to this, the loads could be most easily understood when plotted against flexion angle as in Figure 31. In a general sense, the load varied between two levels: a higher level around 20 Lbs during flexion and a lower load around 10 Lbs during extension. The control deteriorated during the highest extension, this is probably because the moment arms were small in this region. The moment arms are just another sort of gain and when they varied so did system performance.

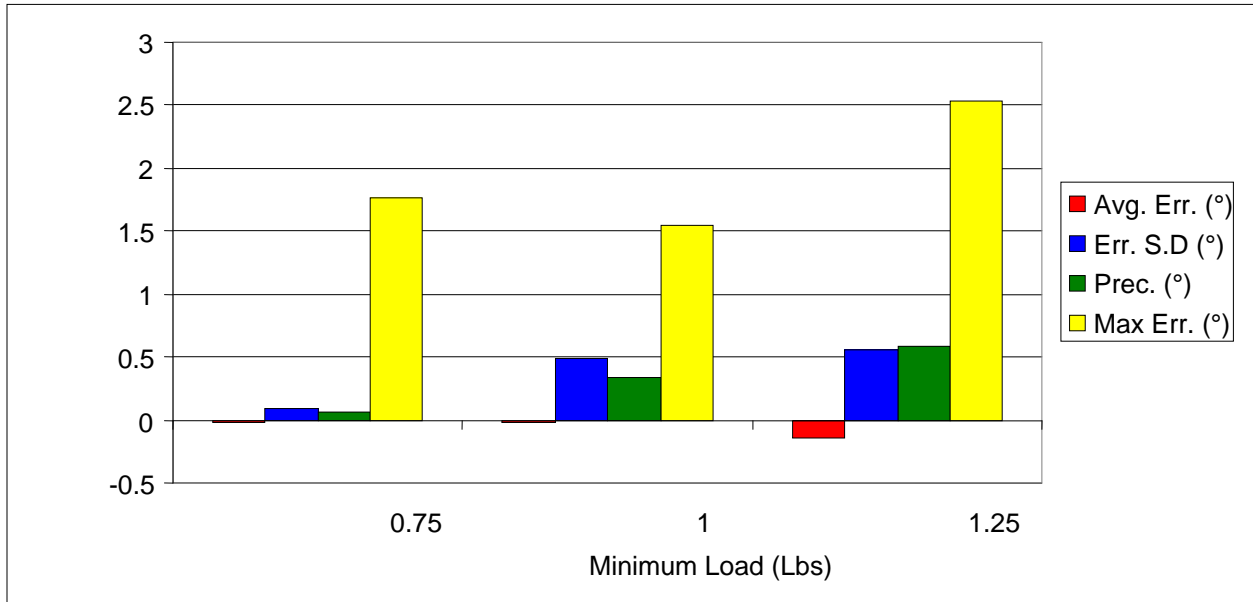


Figure 28. Effects of minimum biceps and pronator teres loads on P/S tracking

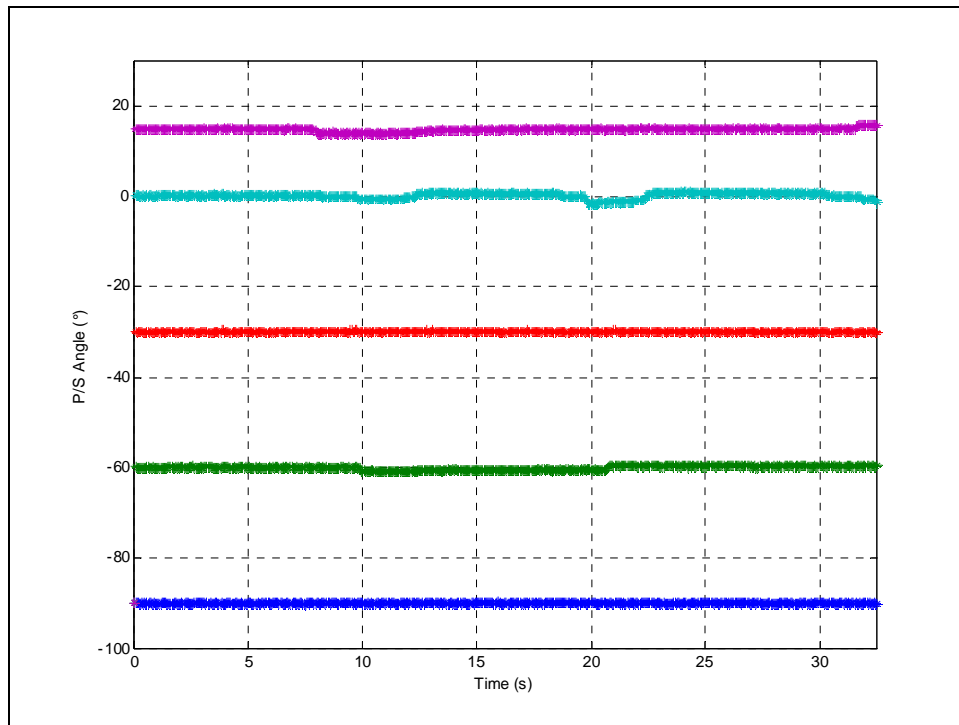


Figure 29. Examples of various constant P/S angles during F/E tests

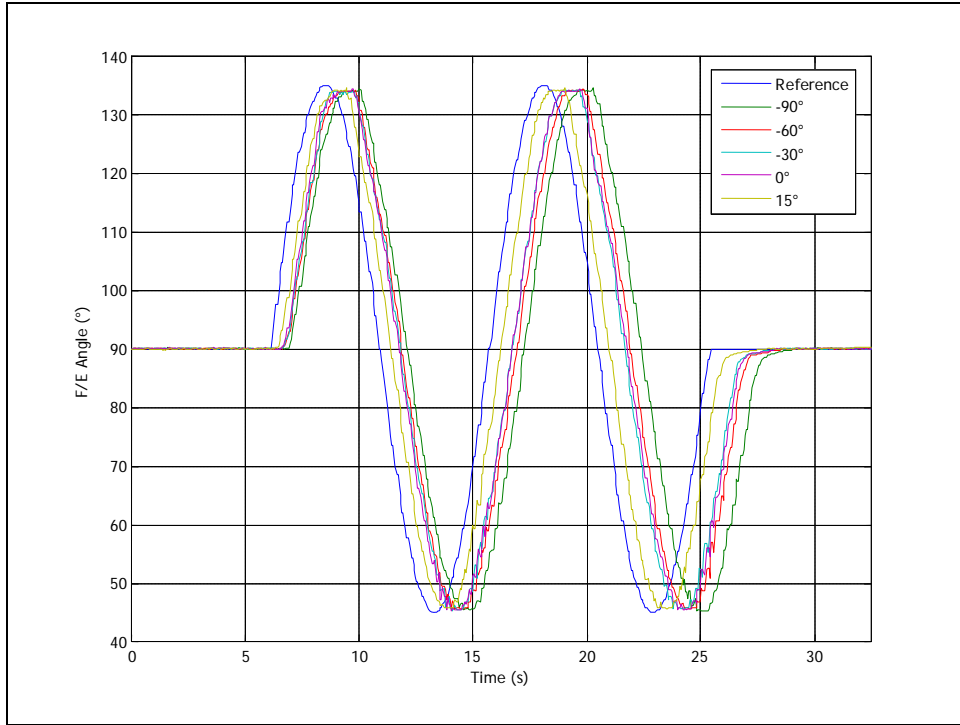


Figure 30. F/E tracking while holding various P/S angles constant

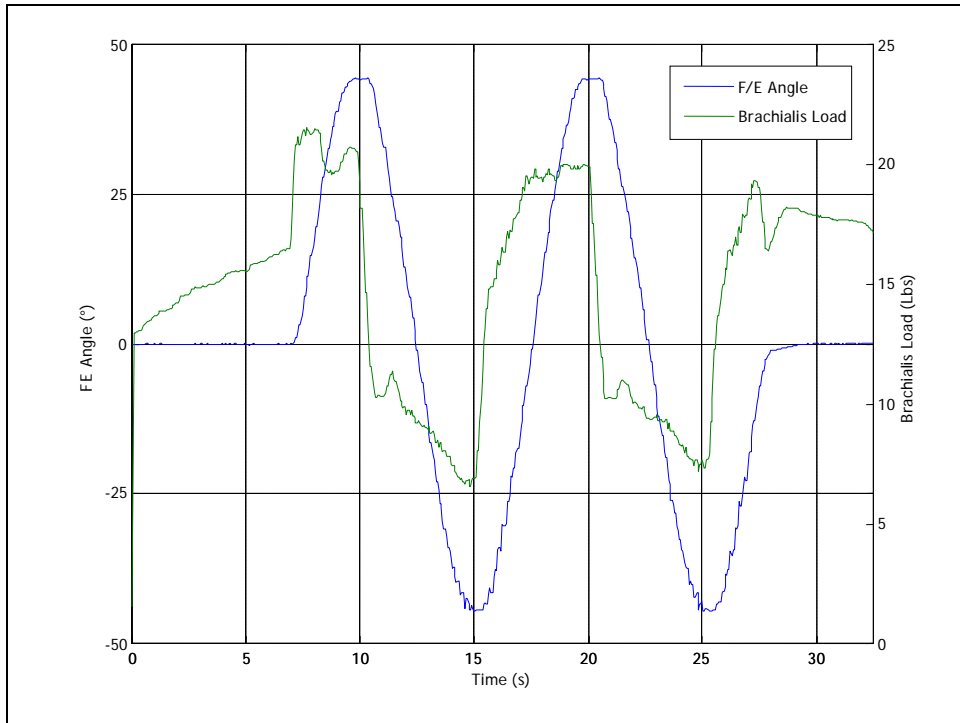


Figure 31. Loading in brachialis tendon during F/E

It is also interesting to look at the biceps and pronator teres loads that are required to maintain the P/S angle. Figures 32 and 33 provide illustrations of these forces from a typical trial along with the reference loads calculated by the controller. The fact that both of these actuators had a flexion moment arm is clear. When the arm flexed and slack needed to be taken up, the loads dropped below the reference, when the arm extended and slack needs to be provided, the loads rose above the reference level.

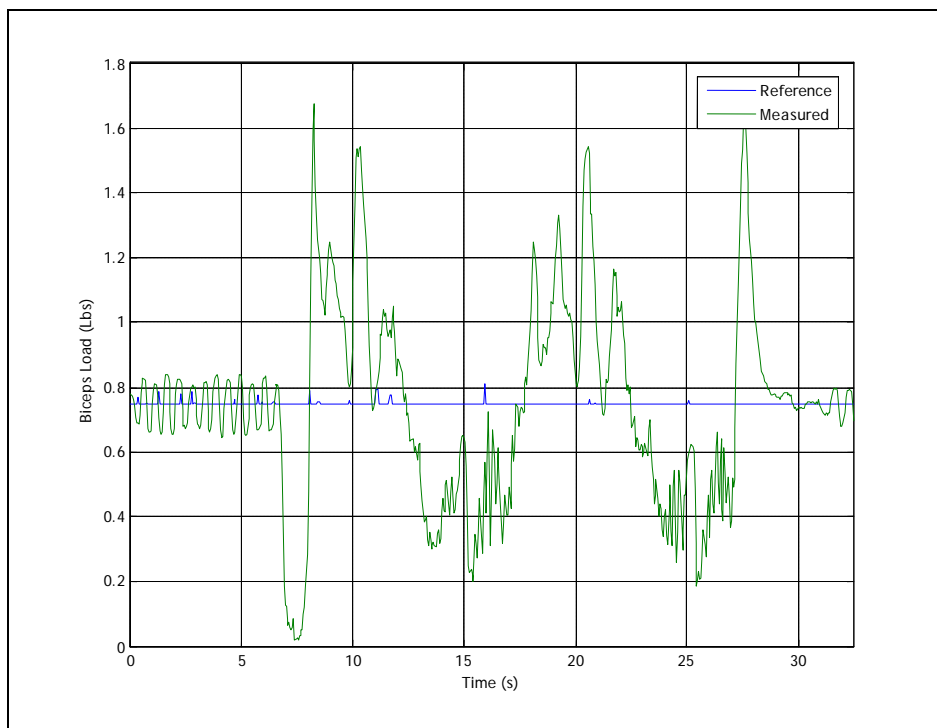


Figure 32. Biceps loads during a typical F/E trial

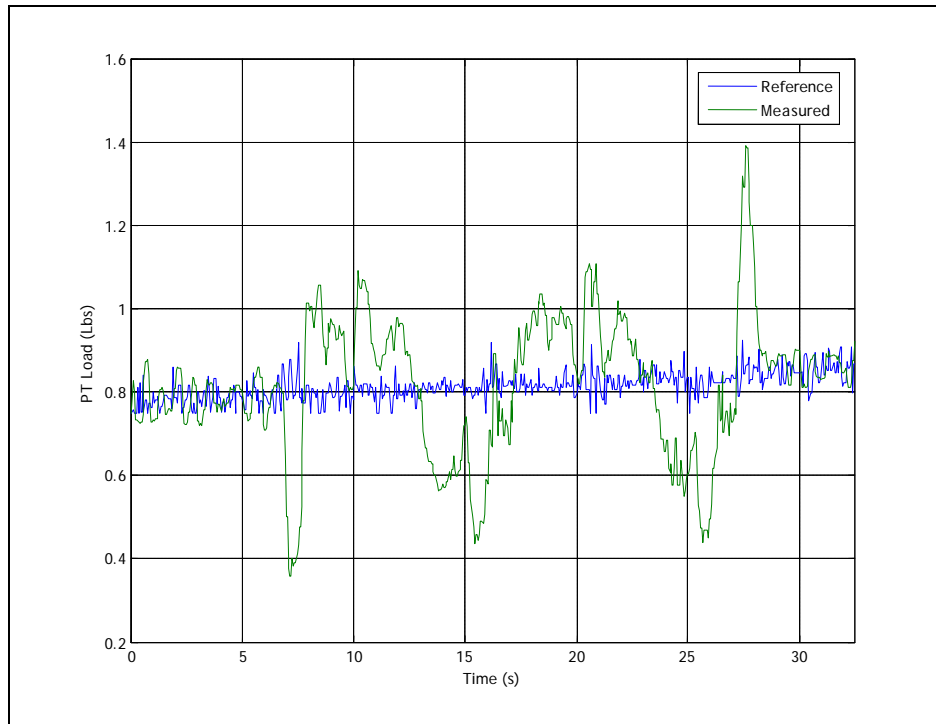


Figure 33. Pronator Teres loads during a typical F/E trial

4.3.2 P/S at Constant F/E Angle

The second test involved evaluating the system’s ability to perform P/S movements at a constant F/E angle; these tests parallel the previous tests. The arm was pronated between -90° and 30° at F/E angles of 55° , 90° , and 135° . Again, the most important part of the test was not the tracking of the P/S signal, but the maintenance of the fixed F/E angle. Again triceps loads were varied between 8, 12, and 16 Lbs and minimum biceps and pronator teres loads were varied between 0.75, 1, and 1.25 Lbs.

The chart in Figure 34 shows the effects of varying the constant flexion angle for the P/S tests. The gains for the system were tuned at 90° , so it makes sense that the performance was best here. Although the current gains were kept the same to isolate the effects of a single variable, during normal testing each individual test could have its own set of optimal gains. This

is also where having a model that could be optimized would be extremely valuable. Trying to vary over a dozen gains by trial and error and clearly understand the effects with each variation is nearly impossible. The errors at 90° and 55° are acceptable; in the future it would be desirable to minimize the maximum error and standard deviation of that error at 135°. This error may in part be due to the poor moment arms that the brachialis and triceps have at this position which make maintaining F/E more difficult.

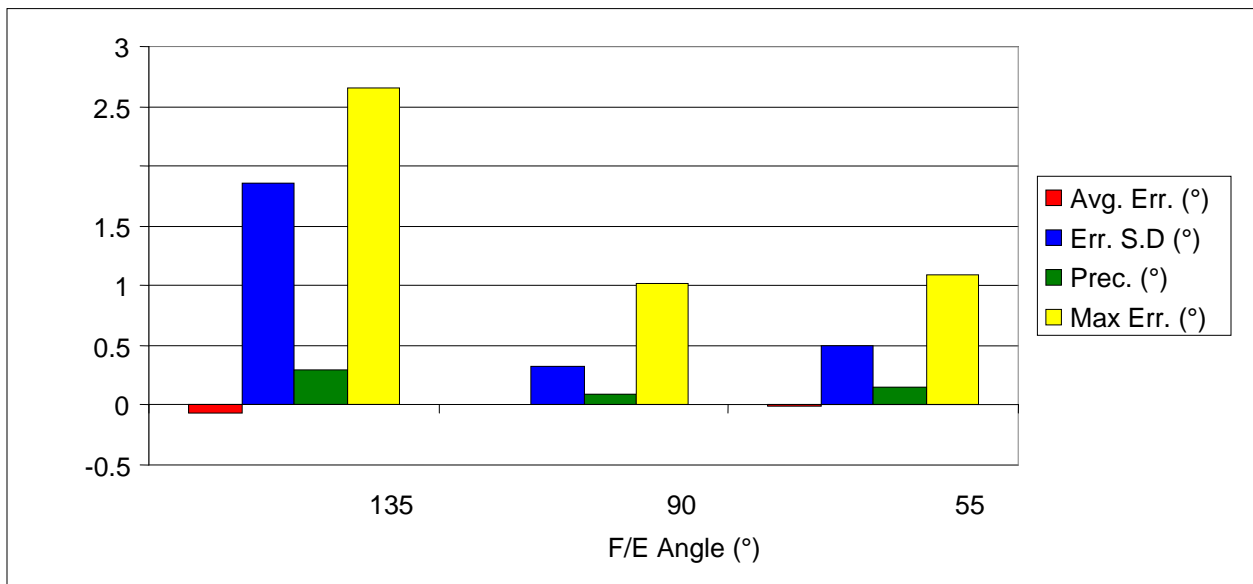


Figure 34. Effects of varying the F/E angle on maintaining a constant F/E angle during P/S

Figure 35 illustrates typical F/E profiles at various F/E angles. The errors occur at the changes in P/S direction. As the biceps go from lower to higher loads or vice versa to change P/S direction, its contribution to the flexion moment also changes so the brachialis is required to vary its loading to maintain a certain F/E angle. If this is not extremely fast, F/E error will occur. This effect can be reduced but not eliminated with this type of system because a servo loop does not predict required loads; it only reduces error once it exists.

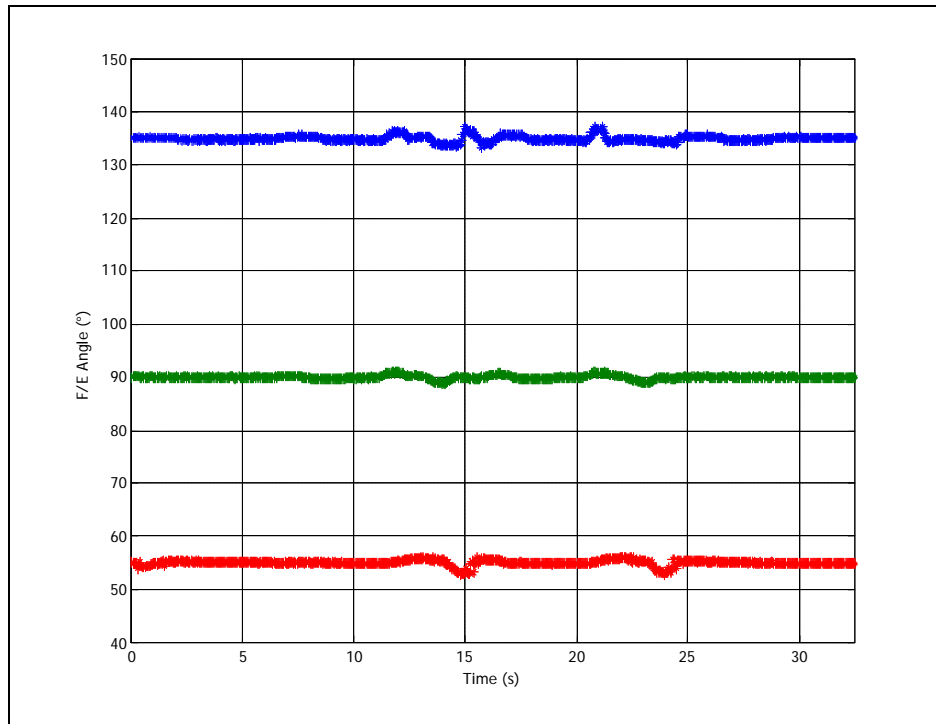


Figure 35. Constant F/E angle during P/S trials

Similar to the previous tests, varying the triceps loading had little effect. Varying the minimum biceps and pronator teres load had little effect on the motion performance, but did influence the accuracy of the biceps load control as shown in Figure 36. The maximum error and the standard deviation of the error were both reduced as the load was reduced.

Figure 37 shows typical P/S tracking trials. The apex of the motion seems to be held longer than it should be. This is due to the transition from pronation to supination. The integral gain in the controller may be at fault. The integral action gives the control signal a sort of inertia due to its time history so it takes a certain amount of time to reduce the momentum of the control signal. Until this happens the system supplements the pronator teres load, not the biceps load, so it does not switch back to supination. Not using integral gain seems to be a simple solution;

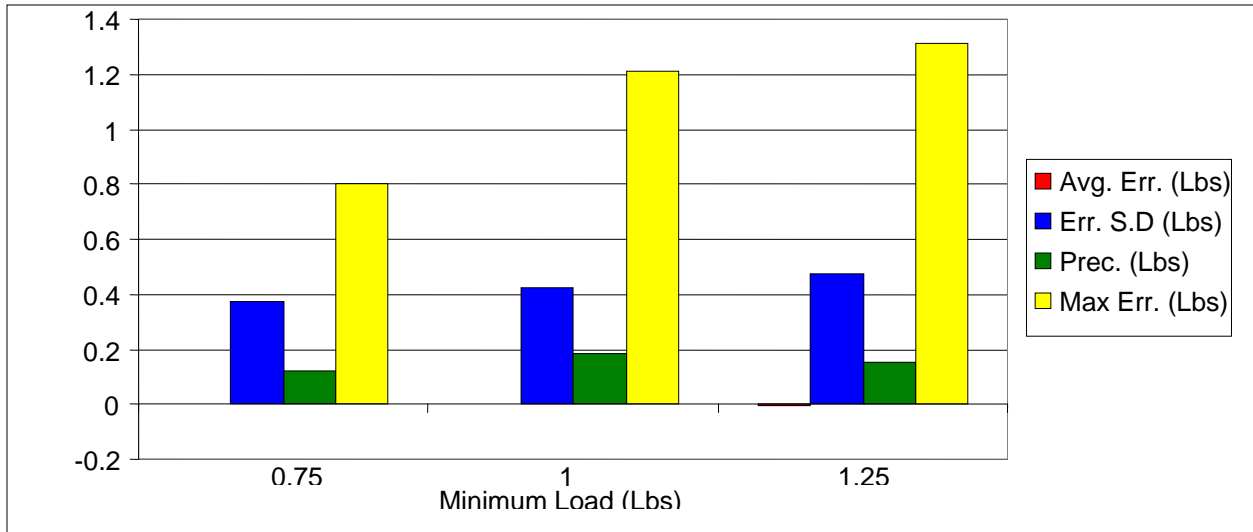


Figure 36. Effects of minimum biceps and pronator teres load on biceps load control

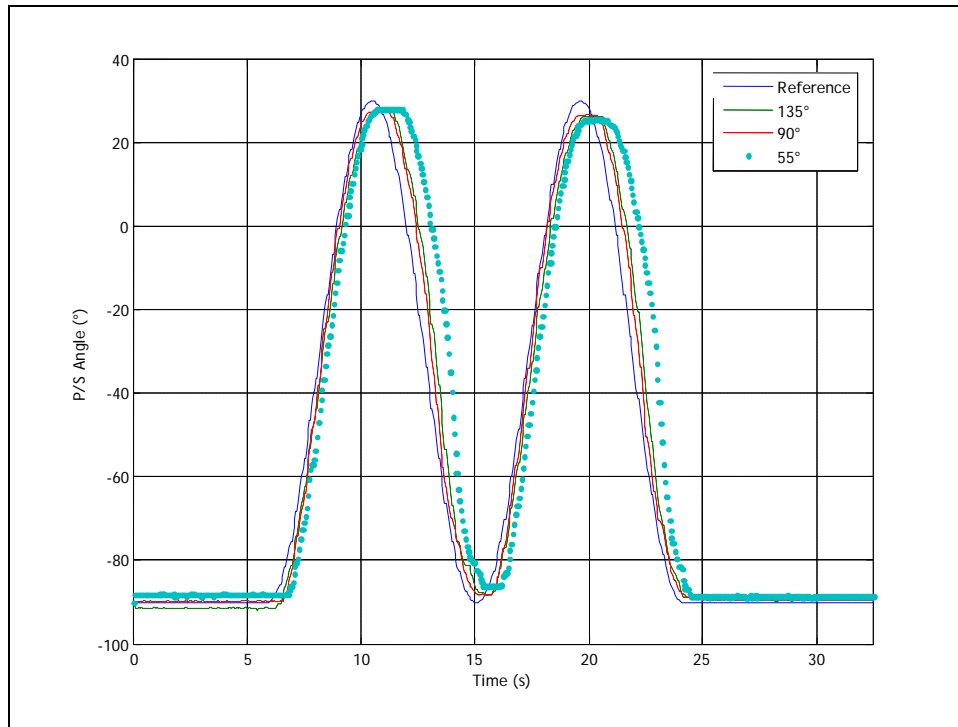


Figure 37. P/S tracking at various constant F/E angles

however, its benefits in steady-state error and the stabilizing effect of that previously mentioned momentum outweigh its shortcomings.

Figures 38 and 39 provide typical examples of biceps and pronator teres loads during P/S. What is most interesting to note is the opposing behavior of the system at around 10 seconds. In very short periods of time the actuators pull back and forth, but because of phase differences, probably due to the order of execution in the code, the biceps and pronator teres are pulling hard out of phase. If they were both pulling hard at the same time there wouldn't be a problem, but in this case their oscillations are slightly offset. If the gains are higher or the controller is slower, these oscillations have a tendency to grow and destabilize the system. This requires acceptance of what seems to be less than great load control with the present system.

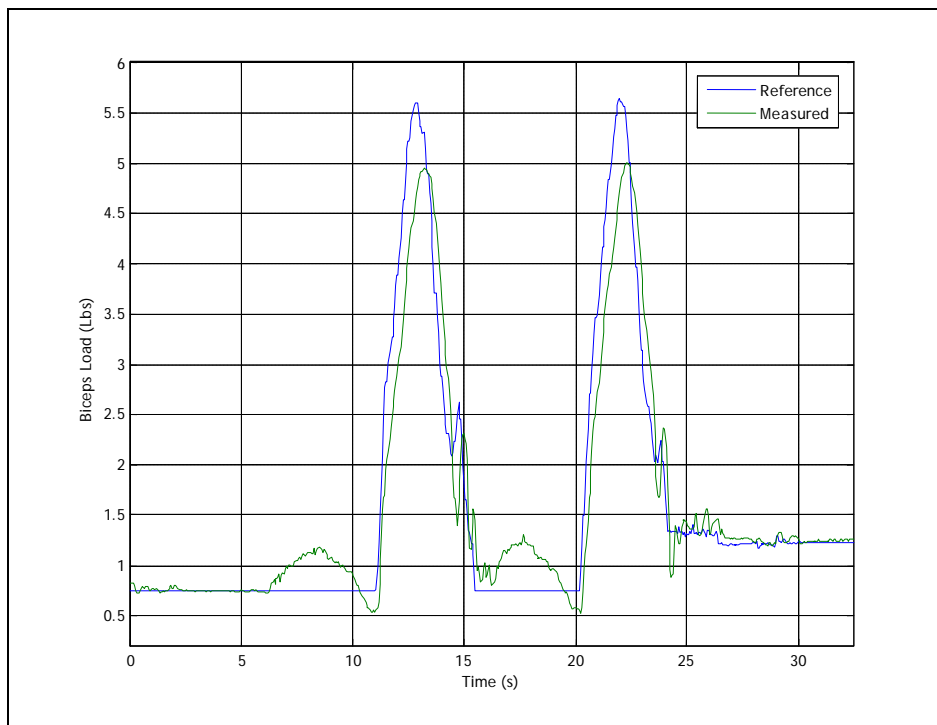


Figure 38. Typical biceps loads during a P/S trial

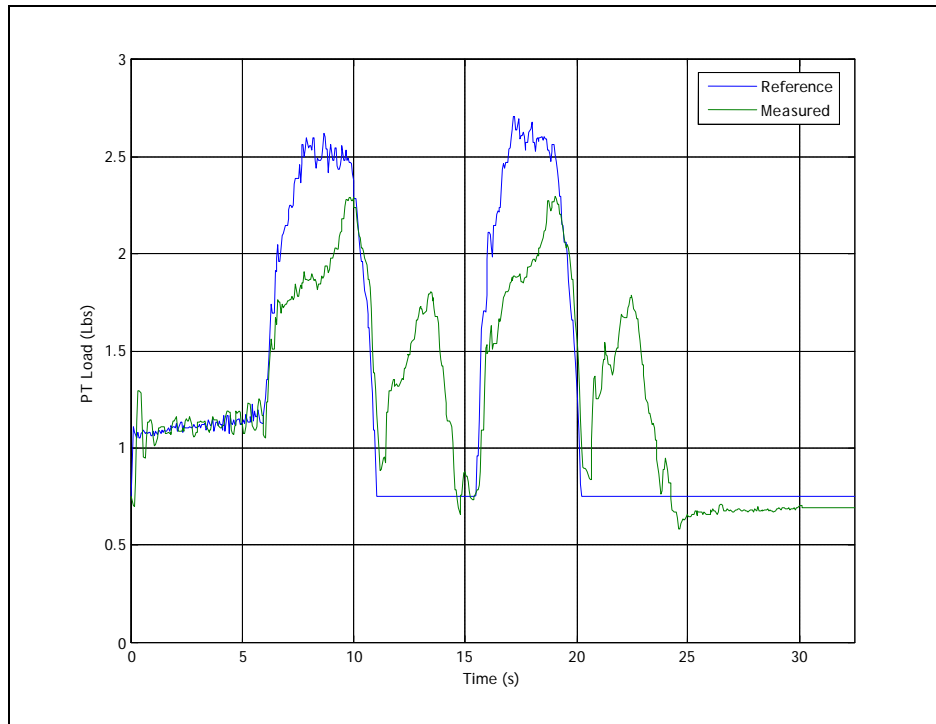


Figure 39. Typical pronator teres loads during a P/S trial

4.3.3 Preliminary Concurrent Motions

Although it was not one of the goals of the project, preliminary concurrent F/E and P/S results were obtained. It is important to note that the period of the motion was increased from 10 seconds to 20 seconds. At the time of testing, an appropriate set of gains had not yet been found to perform the concurrent motions with the 10 second period. The performance measures reported in Figure 40 show that performance at the slower speed is acceptable. The standard deviation of the error and the maximum error show a need for improvement as it is relatively high during P/S. This is probably due to the fact that the P/S control is being performed by actuators that are coupled not only to the degree of freedom they control, but also to another degree of freedom that provides slack in extension and extra tension in flexion. Figure 41 provides an illustration of a concurrent motion trial. The biggest error occurs at the change in

direction of the P/S axis. Again this is probably due to the momentum of the integral action of the PID controller. Work with the gains may bring this down. Also it should be noted that in Figure 41, the Y-Axis markers are deviations from full supination (-90°) and horizontal flexion (90°).

Because of the slower period, the load control on the biceps and pronator teres is improved from previous cases as can be seen in Figures 42 and 43. The general profiles of these two forces are dominated by their roles in P/S. The biceps' load is highest during the second half of the motion when supination occurs and the pronator teres' load is highest during the first half of the motion when pronation occurs.

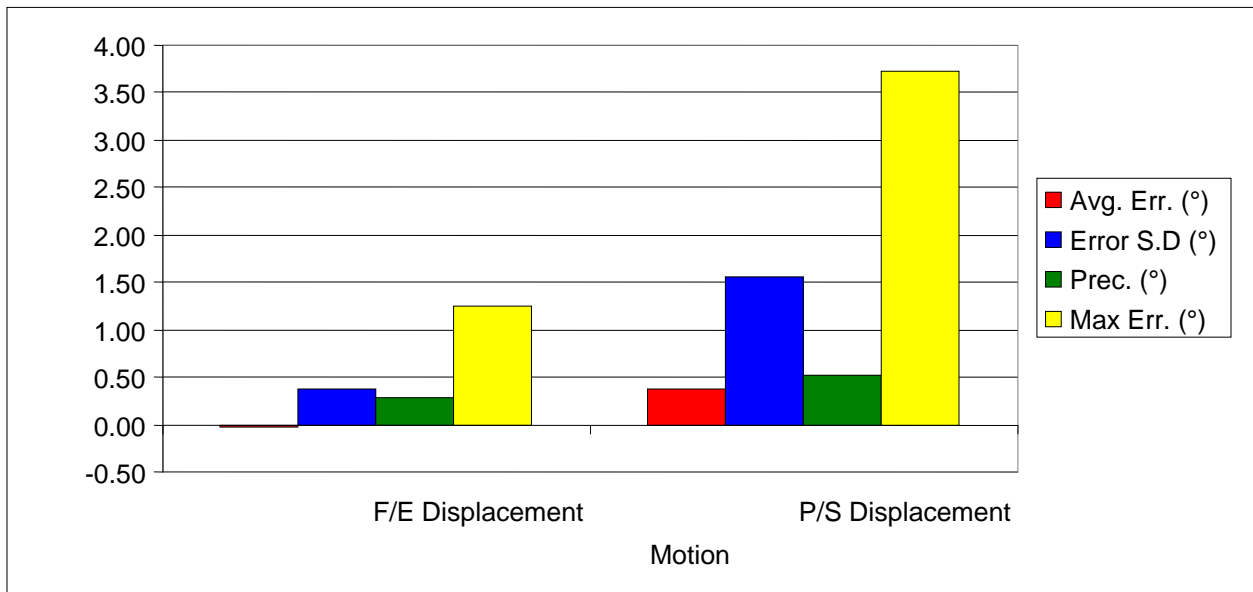


Figure 40. Displacement control performance of concurrent motion controller

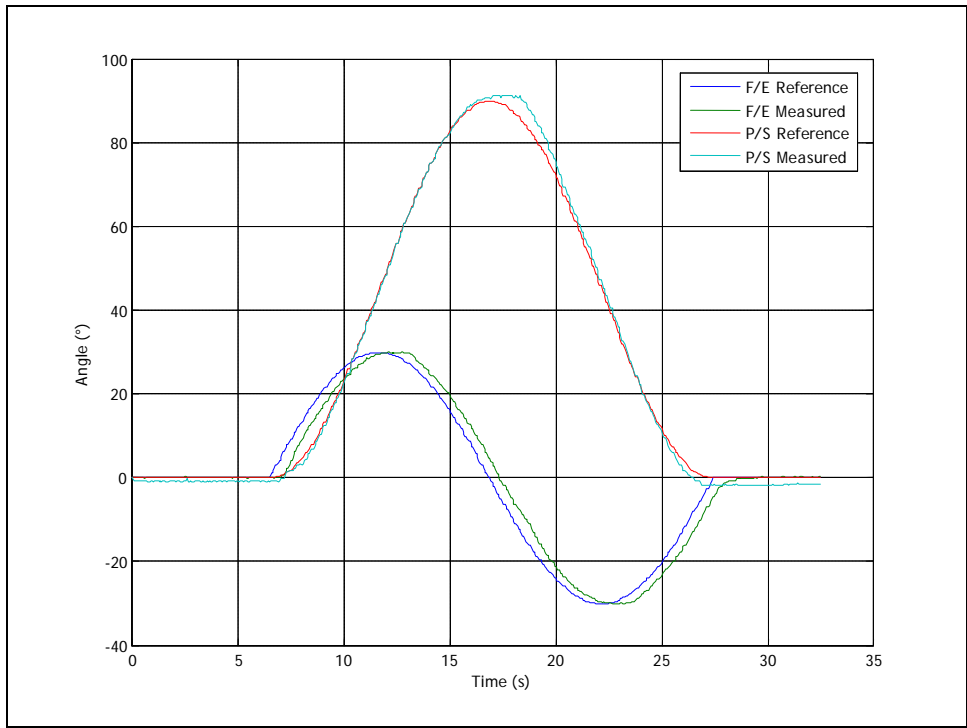


Figure 41. Concurrent F/E and P/S displacement

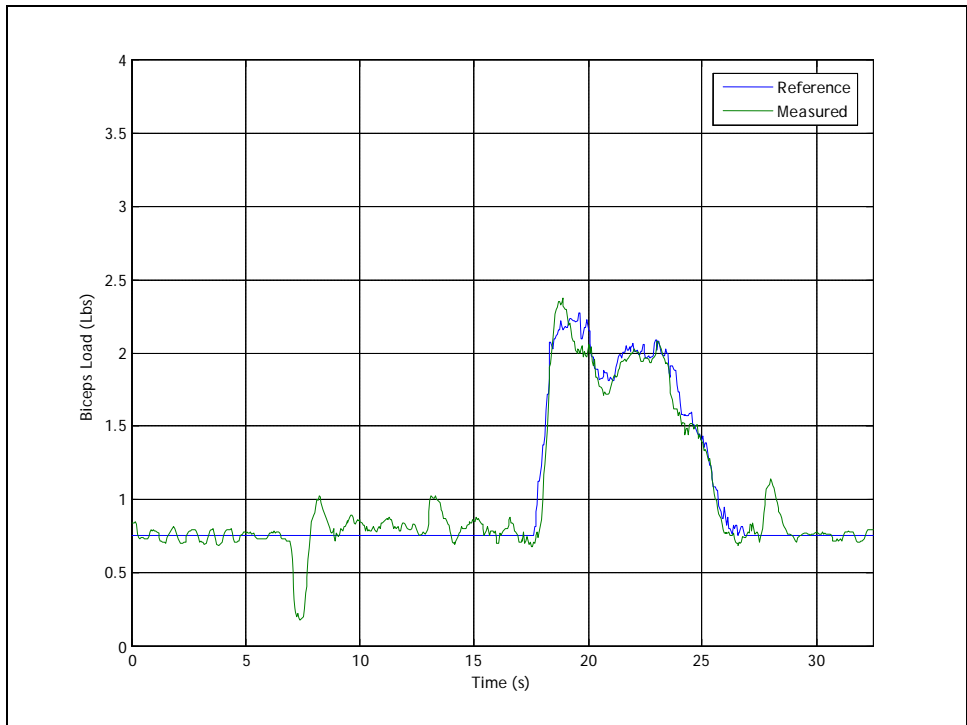


Figure 42. Loading in biceps tendon during concurrent motion

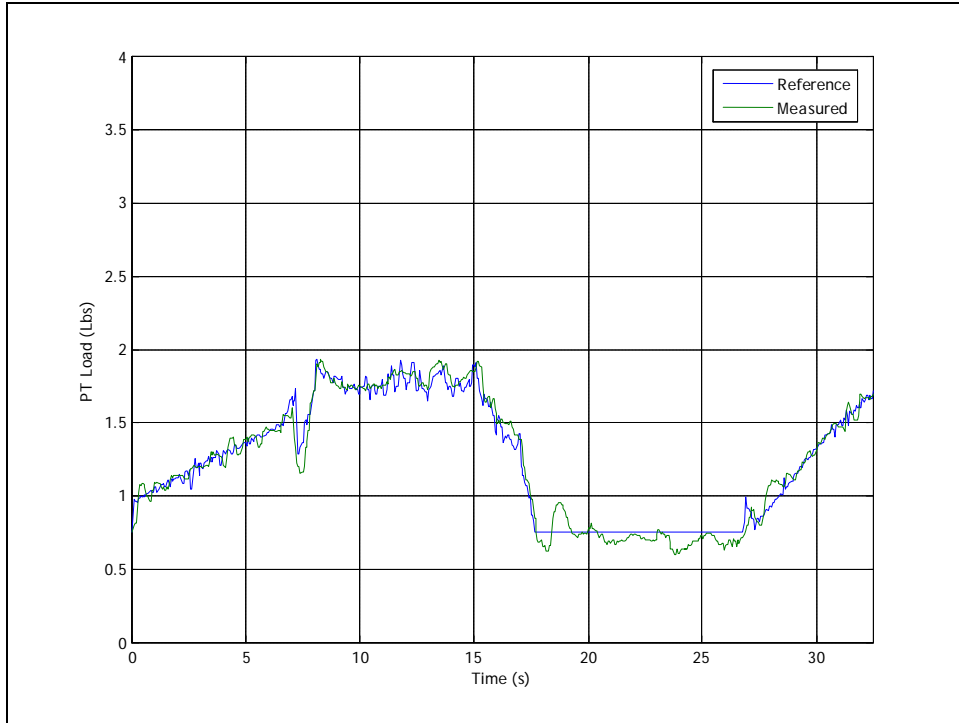


Figure 43. Pronator teres loads during concurrent motion

4.4 KEY LIMITATIONS

During testing, two key system limitations arose: a significant delay between software execution and hardware execution and the inability to set interrupts preventing a constant control loop frequency.

Figure 44 presents data comparing the bit status within the controller with the position of the actuator. The bit status change indicates software execution and the first peak in the bottom plot implies physical movement. Figure 45 shows that the delay also exists when the system is commanded to change velocity, not just starting from a stop.

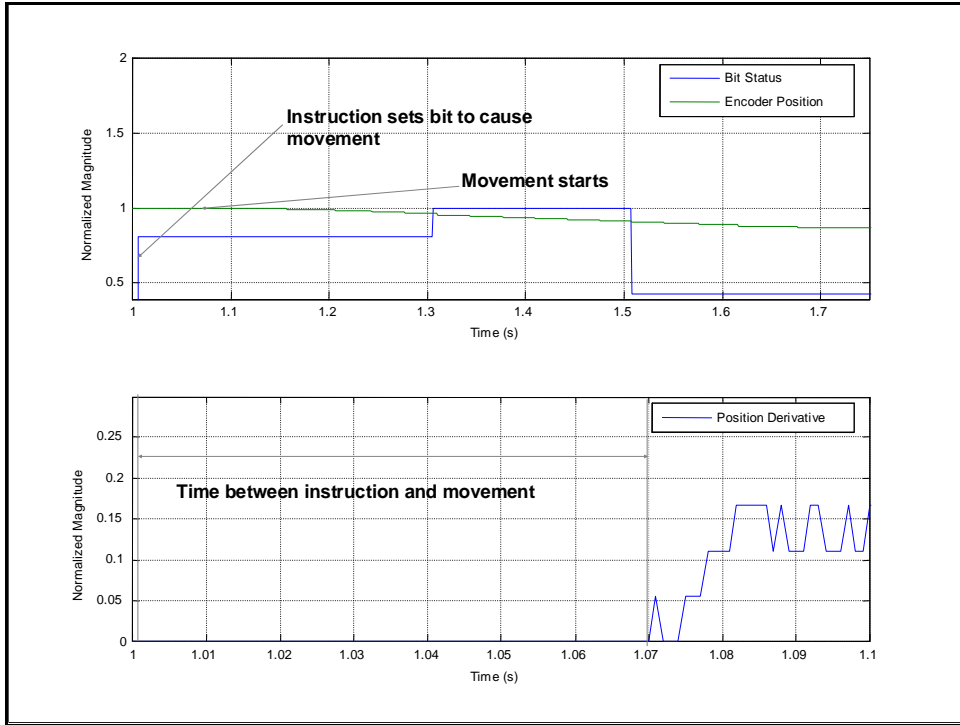


Figure 44. Bit status and encoder position versus time along with the derivative of the encoder position

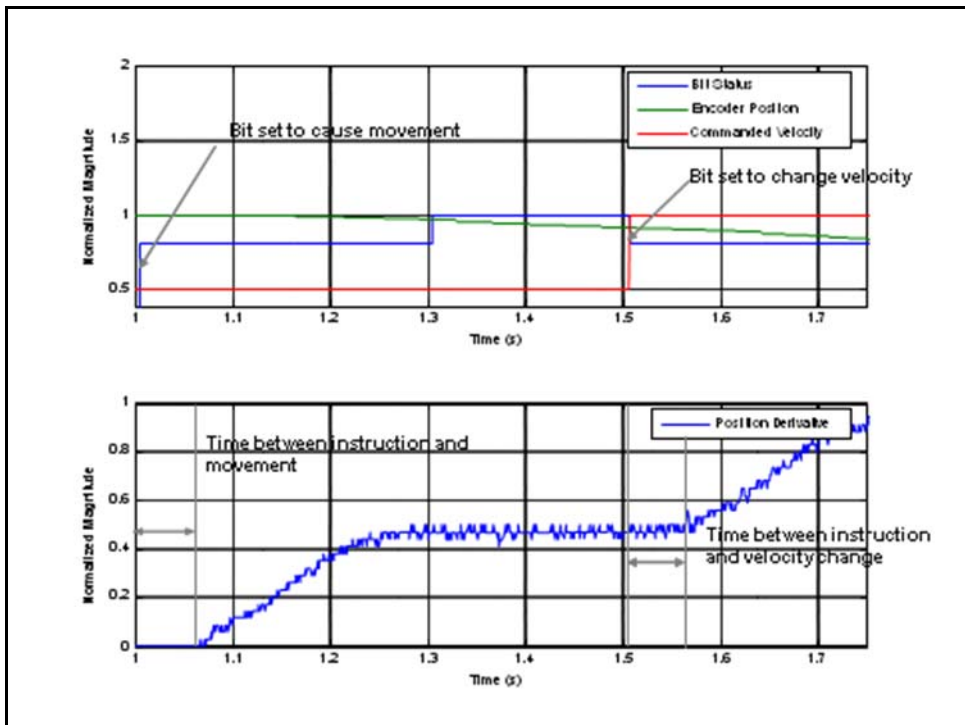


Figure 45. Bit status and encoder position versus time along with the derivative of the encoder position

This delay was important as it puts an immediate upper limit on the bandwidth regardless of any other parameter. Skogestad and Postlethwaite [46] provide a crossover frequency bound, the point at which the gain of the system drops below one:

$$\omega_c < \frac{1}{\theta}$$

In this case theta represents the delay in seconds and omega is the upper bandwidth limit. Using the crossover frequency as a bandwidth limit is used in practice sometimes because it is simple to compute and generally falls between other bandwidth measurements such as those dealing with the sensitivity function and the complementary sensitivity function. Considering this equation, the upper bandwidth limit of this system with a delay of 0.07 seconds is approximately 14.3 Hz. It should be noted that the system is nonlinear and this equation relates to linear systems, so it can only be used as an approximation.

As already mentioned, the control loop's period was a function of code length. If the code is short enough, the system could run faster than the 14.3 Hz mentioned above. In this case, it was necessary to add delays to the end of the code to make the time between command and execution shorter than the time between changes in the control output. If this was not the case, some control signals would never be applied.

Another problem noticed during testing was that of variable controller frequency: the time it took for the system to sample the inputs, compute the appropriate control signals, and then output those signals to the actuators varied. This may be caused by the varying length of different branches within the control code and the inability to set interrupts.

Variable controller frequency can create a sort of variable gain relative to each control loop. For instance, if the controller outputs a signal to move one of the actuators at a given speed for a loop of a certain length, the displacement would equal the product of the speed and the loop

time. If that same speed is output for the next control loop, but the loop itself took twice as long, the system would move twice as far. Relative to control sample rate, the second case would appear to have a gain twice as high as the first even though they were actually the same. Figure 46 provides data illustrating the various lengths of the control loop over the course of ten samples. This result makes it impossible to predict exactly how the system will behave because any sort of disturbance or varying initial condition could cause the system to take a different path through the control algorithm. This puts an unquantifiable limit on the repeatability and also makes the bandwidth variable.

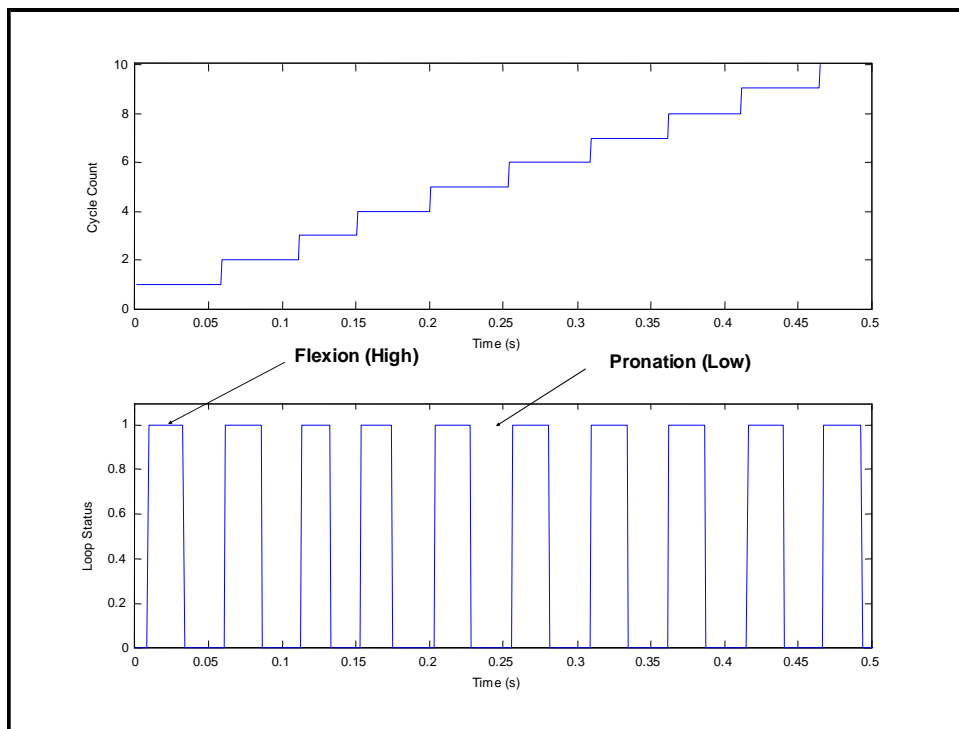


Figure 46. Illustration of the variable length of control cycles due to the inability to control an interrupt

5.0 CONCLUSIONS AND FUTURE WORK

5.1 ACCOMPLISHMENTS

In conclusion, a system has been designed that performs the two desired tests of P/S at a fixed F/E angle and F/E at a fixed P/S angle. Requirements were met to consider the control design a success. The system tracked the desired trajectories to a satisfactory degree based on the measures used to quantify its performance. Also, the system prevented locked conditions by making the biceps and pronator teres compliant to extension. In the same vein, the system prevented slack conditions during flexion where the biceps and pronator teres would have had no tension at all due to their flexion moment arms. Both of these goals were achieved while tracking a desired position with a mixture of load and displacement control. This mixture of load and displacement control also provided joint stability in spite of the uni-directional cable actuation which can only provide forces in the direction of cable tension.

During the testing, it was also found that the triceps loads had very little effect on the performance of the system as long as they were held relatively constant. In general, lower loads seemed to be more attractive because they put less stress on the hardware and are seemingly more like the body, which from common experience does not have large antagonistic loads as it would be inefficient.

Contrary to the triceps loads, the lower limit for the biceps and pronator teres seemed to have an impact on both tracking and the attainment of the desired loads in those actuators. In all cases, the lower the loading, the better the performance.

5.2 FUTURE WORK

Ideally, the system would have been able to perform the trials with a period faster than ten seconds. The system was not ideal for multi-axis feedback control due to the inherent delays between command and execution and the varying rate at which the control algorithm ran.

These problems lead directly to the suggestions for future work which should include the replacement of the controller with a DSP based controller designed to handle real-time multi-axis feedback control. Prior to the acquisition of such a controller, effort should be put forth in deciding the final sensor and actuator goals. Obviously this is not a simple decision, but in an effort to minimize hardware complexity, a ceiling for necessary inputs and outputs would be ideal so that one controller could do all of the work. In the future, various people using the system will not necessarily be familiar with programming or control engineering therefore the interface of the control system should be an important feature in order to make the control algorithm accessible and signal flow intuitive.

As already mentioned in the reference to the work by Stroeve, there should be an effort to mix feedforward control into the system. An appropriate controller would also provide the ability to use feedback as a means for having the feedforward model adapt to desired inputs in the case of a model reference adaptive controller.

APPENDIX A

CONTROLLER CODE

Flexion / Extension Controller Code

PROGRAM

'Program 0

'Variables

Dim SA(4)

Dim SA0(500)

Dim SA1(500)

Dim SA2(500)

Dim SA3(500)

Dim LA(2)

Dim LA0(500)

Dim LA1(500)

Dim SV(55)

'ADC - Analog to Digital Inputs On

ADC ON

'Sampling Variable Initializations

Samp Clear

'A - Flexion Angle Reference

Samp0 SRC SV1

Samp0 Base SA0

'B - Potentiometer Flexion Angle

Samp1 SRC SV2

Samp1 Base SA1

'C - Encoder Y

Samp2 SRC P6160
Samp2 Base LA0

'D - Encoder A
Samp3 SRC P6192
Samp3 Base LA1

'E - Load Cell Triceps Force
Samp4 SRC SV11
Samp4 Base SA2

'F - Load Cell Brachialis Force
Samp5 SRC P6488
Samp5 Base SA3

'Sampling Period (Milliseconds)
P6915 = 50

'Counter
SV0 = 1

'Flexion Displacement Values

SV1 = 0
SV2 = SV1
SV3 = 0
SV4 = 0
SV5 = 0
SV6 = 0
SV7 = 0.175
SV8 = 0
SV9 = 0

'Triceps Force Values (A - Axis)

SV10 = 8
SV11 = SV10
SV12 = 0
SV13 = 0
SV14 = 0
SV15 = 0
SV16 = 0.3
SV17 = 0
SV18 = 0

'Brachialis Force Values (Y - Axis)

'SV19 is the minimum Brachialis force
SV19 = 1.5

SV20 = SV19
SV21 = 0
SV22 = 0
SV23 = 0
SV24 = 0
SV25 = 0.1
SV26 = 0.0015
SV27 = 0

'Error Values - Two Samples Previous

SV28 = 0
SV29 = 0
SV30 = 0

'Sampled Program

Set 105

'Jog Velocities Zero

P12348 = 0
P12604 = 0
P12860 = 0
P13116 = 0

'Control Loop

While (SV0 < 1220)

.....

'Displacement Control - Outer Loop

If (SV0 <= 100)

SV1 = 0

Else If (SV0 <= 1120)

SV1 = 30*SIN(360*(SV0-100)/510)

Else

SV1 = 0

EndIf

SV2 = P6456

SV3 = SV2 - SV1

SV5 = SV6 + (SV7 + SV8 + SV9) * SV3 - (SV7 + 2 * SV9) * SV4 +
(SV9) * SV28

If (P6488 >= SV19)

If (SV5 > 0)

Set 828

Else If (SV5 < 0)

```
        Set 829
    Else
        Clr 828
        Clr 829
    EndIf
```

$P12604 = SV7 * \text{Absf}(SV5)$

'Triceps Force Control - Inner Loop #1

SV11 = P6520

SV12 = SV11 - SV10

SV14 = SV15 + (SV16 + SV17) * SV12 - SV16 * SV13

If (SV14 > 0)

Set 892

Else If (SV14 < 0)

Set 893

Else

Clr 892

Clr 893

EndIf

$P13116 = SV16 * \text{Absf}(SV14)$

SV13 = SV12

SV15 = SV14

Else

If (SV5 > 0)

Set 893

Else If (SV5 < 0)

Set 892

Else

Clr 893

Clr 892

EndIf

$P13116 = SV7 * \text{Absf}(SV5)$

'Brachialis Force Control - Inner Loop #2

SV20 = P6488

SV21 = SV20 - SV19

SV23 = SV24 + (SV25 + SV26) * SV21 - SV25 * SV22

```
If (SV23 > 0)
    Set 828
Else If (SV23 < 0)
    Set 829
Else
    Clr 828
    Clr 829
EndIf
```

```
P12604 = SV25 * Absf(SV23)
```

```
SV22 = SV21
SV24 = SV23
```

```
EndIf
```

```
SV4 = SV3
SV6 = SV5
SV28 = SV4
```

```
.....
' Counter Increment
    SV0 = SV0 + 1
```

```
Wend
```

```
'Stop Movement
P12348 = 0
Clr 796
Clr 797
```

```
P12604 = 0
Clr 828
Clr 829
```

```
P12860 = 0
Clr 860
Clr 861
```

```
P13116 = 0
Clr 892
Clr 893
```

```
'Stop Sampling
INH -105
```

ENDP

Code for Final controller

```
PROGRAM
'Program 0

'////////////////////////////////////
' Variable Initialization

' Number of Array Variables
Dim SA(8)
Dim LA(1)

'Array Variable Length
Dim SA0(650)
Dim SA1(650)
Dim SA2(650)
Dim SA3(650)
Dim SA4(650)
Dim SA5(650)
Dim SA6(650)
Dim SA7(650)
Dim LA0(650)

'Number of Scalar Variables
Dim SV(72)

'ADC - Analog to Digital Inputs On
ADC ON

'////////////////////////////////////
' Sampling Setup

'Sampling Variable Initializations
Samp Clear

'A - Sinusoidal Reference
Samp0 SRC SV1
Samp0 Base SA0

'B - Inclinator Flexion Angle
Samp1 SRC SV2
Samp1 Base SA1

'C - Potentiometer Pronation Angle
```

Samp2 SRC SV29
Samp2 Base SA2

'D - Triceps Load
Samp3 SRC SV11
Samp3 Base SA3

'E - Load Cell Biceps Force
Samp4 SRC P6472
Samp4 Base SA4

'F - Biceps Reference
Samp5 SRC SV60
Samp5 Base SA5

'G - Load Cell PT Force
Samp6 SRC SV47
Samp6 Base SA6

'H - PT Reference
Samp7 SRC SV61
Samp7 Base SA7

'Sampling Period (Milliseconds)
P6915 = 50

//

' CPU Period Setup
Period 0.001

//

' Acceleration Levels
Jog Acc X3000
Jog Dec X3000

Jog Acc Y3000
Jog Dec Y3000

Jog Acc Z3000
Jog Dec Z3000

Jog Acc A3000
Jog Dec A3000

//

' Counter Initialization

SV0 = 1

//

' Pattern for Control Values

- ' 1 = Reference
- ' 2 = Current State
- ' 3 = Error Signal
- ' 4 = Previous Error
- ' 5 = Control Signal
- ' 6 = Previous Control Signal
- ' 7 = Proportional Gain
- ' 8 = Integral Gain
- ' 9 = Derivative Gain
- ' 10 = 2x Previous Error

//

' Pattern for Control Values

- ' 1 = Reference
- ' 2 = Current State
- ' 3 = Error Signal
- ' 4 = Previous Error
- ' 5 = Control Signal
- ' 6 = Previous Control Signal
- ' 7 = Proportional Gain
- ' 8 = Integral Gain
- ' 9 = Derivative Gain
- ' 10 = 2x Previous Error

//

' Flexion Displacement Values

- SV1 = 0
- SV2 = SV1
- SV3 = 0
- SV4 = 0
- SV5 = 0
- SV6 = 0
- SV7 = 0.04
- SV8 = 0
- SV9 = 0.01
- SV55 = 0

//

' Triceps Force Values (A-Axis)

SV10 = 8
SV11 = SV10
SV12 = 0
SV13 = 0
SV14 = 0
SV15 = 0
SV16 = 0.8
SV17 = 0.07
SV18 = 0
SV56 = 0

////////////////////////////////////
'Brachialis Force Values (Y - Axis)

SV19 = 1.5
SV20 = SV19
SV21 = 0
SV22 = 0
SV23 = 0
SV24 = 0
SV25 = 0.1
SV26 = 0.0005
SV27 = 0
SV57 = 0

////////////////////////////////////
'Pronation Displacement Values

SV28 = 0
SV29 = SV28
SV30 = 0
SV31 = 0
SV32 = 0
SV33 = 0
SV34 = 0.4
SV35 = 0.008
SV36 = 0.006
SV58 = 0

////////////////////////////////////
'Biceps Force Values (X - Axis)

SV37 = 0.75
SV38 = SV37
SV39 = 0

SV40 = 0
SV41 = 0
SV42 = 0
SV43 = 0.3
SV44 = 0.06
SV45 = 0.002
SV65 = 0

////////////////////////////////////
'Pronator Teres Force Values (Z - Axis)

SV46 = 0.75
SV47 = SV46
SV48 = 0
SV49 = 0
SV50 = 0
SV51 = 0
SV52 = 0.3
SV53 = 0.06
SV54 = 0.002
SV66 = 0

////////////////////////////////////
'Intermediate Biceps Load
SV60 = SV37

////////////////////////////////////
'Intermediate Pronator Teres Load
SV61 = SV46

////////////////////////////////////
'Start Sampling

Set 105

////////////////////////////////////
'Jog Velocities Zero

P12348 = 0
P12604 = 0
P12860 = 0
P13116 = 0

////////////////////////////////////
'Control Loop

While (SV0 < 500)

////////////////////////////////////

'Displacement Control - Outer Loop

'Denominator 250 for 10s period

////////////////////////////////////

' Flexion Reference Signal

If (SV0 <= 100)

SV1 = 0

Else If (SV0 <= 400)

SV1 = 45*SIN(360*(SV0-100)/150)

SV1 = 0

Else

SV1 = 0

EndIf

////////////////////////////////////

' Sample Sensor / Calculate Error Signal / Control Signal

SV2 = P6456

SV3 = SV2 - SV1

SV5 = SV6 + (SV7 + SV8 + SV9) * SV3 - (SV7 + 2 * SV9) * SV4 +
(SV9) * SV55

SV20 = P6488

SV21 = SV20 - SV19

////////////////////////////////////

If (SV5 > 0)

If (SV21 < 0)

SV11 = P6520

Set 893

P13116 = Absf(SV5)

SV23 = SV24 + (SV25 + SV26 + SV27) * SV21 - (SV25 +
2 * SV27) * SV22 + (SV27) * SV57

Set 829

P12604 = Absf(SV23)

SV57 = SV22

SV22 = SV21

SV24 = SV23

```

SV56 = 0
SV13 = 0
SV15 = 0

Else
Set 828
P12604 = Absf(SV5)

SV11 = P6520
SV12 = SV11 - SV10
SV14 = SV15 + (SV16 + SV17 + SV18) * SV12 - (SV16 +
2 * SV18) * SV13 + (SV18) * SV56

If (SV14 > 0)
Set 892
Else
Set 893
EndIf

P13116 = Absf(SV14)

SV56 = SV13
SV13 = SV12
SV15 = SV14

SV57 = 0
SV22 = 0
SV24 = 0
EndIf

Else

Set 829
P12604 = Absf(SV5)

SV11 = P6520
SV12 = SV11 - SV10
SV14 = SV15 + (SV16 + SV17 + SV18) * SV12 - (SV16 + 2 *
SV18) * SV13 + (SV18) * SV56

If (SV14 > 0)
Set 892
Else
Set 893
EndIf

```

P13116 = Absf(SV14)

SV56 = SV13

SV13 = SV12

SV15 = SV14

SV57 = 0

SV22 = 0

SV24 = 0

EndIf

SV55 = SV4

SV4 = SV3

SV6 = SV5

////////////////////////////////////

'Pronation Error Calculation

'Denominator 250 for 10s period

If (SV0 <= 100)

SV28 = 0

Else If (SV0 <= 400)

SV28 = 60*(COS(360*(SV0-100)/150-180)+1)

SV28 = 0

Else

SV28 = 0

EndIf

SV29 = P6424

SV30 = SV29 - SV28

SV32 = SV33 + (SV34 + SV35 + SV36) * SV30 - (SV34 + 2 * SV36) *

SV31 + (SV36) * SV58

If (SV32 >= 0)

SV60 = SV37 + SV32

SV61 = SV46

Else

SV60 = SV37

SV61 = SV46 - SV32

EndIf

SV58 = SV31

SV31 = SV30

SV33 = SV32

```

////////////////////////////////////
'Pronator Teres Force Control
  SV47 = P6504
  SV48 = SV47 - SV61
  SV50 = SV51 + (SV52 + SV53 + SV54) * SV48 - (SV52 + 2 * SV54) *
SV49 + (SV54) * SV66

  If (SV50 < 0)
    Set 861
  Else
    Set 860
  EndIf

  P12860 = Absf(SV50)

  SV66 = SV49
  SV49 = SV48
  SV51 = SV50

////////////////////////////////////
' Biceps Load Control
  SV38 = P6472
  SV39 = SV38 - SV60
  SV41 = SV42 + (SV43 + SV44 + SV45) * SV39 - (SV43 + 2 * SV45) *
SV40 + (SV45) * SV65

  If (SV41 < 0)
    Set 797
  Else
    Set 796
  EndIf

  P12348 = Absf(SV41)

  SV65 = SV40
  SV40 = SV39
  SV42 = SV41
.....
' Pause
  DWL 0.02

' Counter Increment
  SV0 = SV0 + 1

Wend

```

'Stop Movement
P12348 = 0
Clr 796
Clr 797

P12604 = 0
Clr 828
Clr 829

P12860 = 0
Clr 860
Clr 861

P13116 = 0
Clr 892
Clr 893

'Stop Sampling
INH -105

'Turn Filters Off
ENDP

APPENDIX B

CONTROLLER TESTING RESULTS

Table 1. Performance of F/E controller displacement feedback with various triceps loading

Control Type	Displacement						
Triceps Load	4	6	8	10	12	14	16
Avg. Error	0.07	0.08	-0.08	0.1	0.06	0.11	0
Error S.D	1.13	1.17	1.49	1.11	1.13	1.11	1.04
Avg. Precision	0.67	0.83	1	0.75	0.73	0.65	0.88
Max Error	4.1	4.2	4.69	3.33	3.72	4.77	3.63

Table 2. Performance of F/E controller force feedback with various triceps loading

Control Type	Triceps Load						
Triceps Load	4	6	8	10	12	14	16
Avg. Error	0.02	0	0.01	0.01	0	-0.01	0.01
Error S.D	0.55	0.55	0.55	0.56	0.55	0.56	0.56
Avg. Precision	0.14	0.1	0.12	0.11	0.11	0.1	0.12
Max Error	1.54	1.54	1.28	1.72	1.38	1.42	1.38

Table 3. Performance of F/E controller as triceps loads are varied

Control Type	F/E Displacement			P/S Displacement			Triceps Control		
Triceps Load	8	12	16	8	12	16	8	12	16
Avg. Error	0.07	-0.05	0.07	-0.16	-0.16	-0.02	0.00	0.00	0.00
Error S.D	1.07	1.72	1.06	0.08	0.55	0.09	0.15	0.15	0.15
Avg. Precision	0.76	2.32	1.23	0.06	0.53	0.06	0.05	0.06	0.05
Max Error	4.53	7.45	4.49	0.19	1.83	1.76	0.45	0.51	0.51
Avg. Lag	0.50	0.28	0.38						

Table 4. Performance of F/E controller as biceps and pronator teres minimum loads are varied

Control Type	F/E Displacement			P/S Displacement			Biceps Load Control			PT Load Control		
	0.75	1	1.25	0.75	1	1.25	0.75	1	1.25	0.75	1	1.25
Min Load	0.75	1	1.25	0.75	1	1.25	0.75	1	1.25	0.75	1	1.25
Avg. Error	0.07	-0.03	0.10	-0.02	-0.02	-0.14	0.00	0.01	0.00	0.00	0.00	0.00
Error S.D	1.06	1.09	1.13	0.09	0.49	0.55	0.32	0.39	0.40	0.16	0.19	0.19
Avg. Precision	1.23	2.68	2.68	0.06	0.34	0.58	0.09	0.21	0.21	0.05	0.29	0.31
Max Error	4.49	4.45	7.29	1.76	1.55	2.54	1.36	1.27	1.39	0.58	1.06	0.61
Avg. Lag	0.38	0.68	0.22									

Table 5. Performance of F/E controller as P/S angle is varied

Control Type	F/E Displacement					P/S Displacement				
	-90	-60	-30	0	15	-90	-60	-30	0	15
PS Angle	-90	-60	-30	0	15	-90	-60	-30	0	15
Avg. Error	0.07	0.05	0.15	0.06	-0.14	-0.02	-0.02	0.06	0.13	-0.16
Error S.D	1.06	1.02	1.63	1.38	3.78	0.09	0.49	0.16	0.60	0.41
Avg. Precision	1.23	1.21	2.19	3.04	7.15	0.06	0.14	0.17	0.28	0.22
Max Error	4.49	4.94	8.05	8.11	14.60	1.76	1.52	0.64	2.01	1.82
Avg. Lag	0.38	0.60	0.70	0.33	1.23					

Table 6. Performance of P/S controller as F/E angle is varied

Control Type	F/E Displacement			P/S Displacement			Triceps Control		
	8	12	16	8	12	16	8	12	16
Triceps Load	8	12	16	8	12	16	8	12	16
Avg. Error	0.00	0.00	0.00	-1.21	-1.10	-0.89	0.00	0.00	0.00
Error S.D	0.30	0.31	0.32	2.34	2.29	2.35	0.06	0.05	0.06
Avg. Precision	0.09	0.09	0.10	0.58	0.73	1.87	0.04	0.04	0.05
Max Error	0.95	0.98	1.02	5.86	4.88	5.39	0.34	0.20	0.23
Avg. Lag				0.32	0.35	0.32			

Table 7. Performance of P/S controller as the biceps and pronator teres minimum loads are varied

Control Type	F/E Displacement			P/S Displacement			Biceps Load Control			PT Load Control		
	0.75	1	1.25	0.75	1	1.25	0.75	1	1.25	0.75	1	1.25
Min Load	0.75	1	1.25	0.75	1	1.25	0.75	1	1.25	0.75	1	1.25
Avg. Error	0.00	0.01	0.01	-0.89	-1.78	-2.06	0.00	0.00	0.00	0.01	0.01	0.01
Error S.D	0.32	0.33	0.34	2.35	2.31	2.30	0.37	0.42	0.47	0.42	0.42	0.42
Avg. Precision	0.10	0.10	0.11	1.87	2.21	1.28	0.12	0.18	0.15	0.06	0.08	0.06
Max Error	1.02	1.08	1.05	5.39	3.90	3.94	0.80	1.21	1.31	1.19	1.19	1.26
Avg. Lag				0.32	0.45	0.43						

Table 8. Performance of P/S controller at various F/E angles

Control Type	F/E Displacement					P/S Displacement				
	-90	-60	-30	0	15	-90	-60	-30	0	15
PS Angle	-90	-60	-30	0	15	-90	-60	-30	0	15
Avg. Error	0.07	0.05	0.15	0.06	-0.14	-0.02	-0.02	0.06	0.13	-0.16
Error S.D	1.06	1.02	1.63	1.38	3.78	0.09	0.49	0.16	0.60	0.41
Avg. Precision	1.23	1.21	2.19	3.04	7.15	0.06	0.14	0.17	0.28	0.22
Max Error	4.49	4.94	8.05	8.11	14.60	1.76	1.52	0.64	2.01	1.82
Avg. Lag	0.38	0.60	0.70	0.33	1.23					

Table 9. Performance of controller during a concurrent F/E and P/S motion

Control Type	F/E Displacement	P/S Displacement
Avg. Error	-0.03	0.37
Error S.D	0.38	1.55
Avg. Precision	0.28	0.52
Max Error	1.24	3.73
Avg. Lag	0.48	0.05

BIBLIOGRAPHY

- [1] Morrey BF, 2000, *The Elbow and Its Disorders*, W.B. Saunders Company, Philadelphia, pp. 341-364, Chap. 25.
- [2] Hicks JH, 1953, "The Mechanics of the Foot," *Journal of Anatomy*, **87**(4), pp. 345-357.
- [3] Hicks JH, 1955, "The Foot as a Support," *Acta Anatomica*, **25**, pp. 34-45.
- [4] Shaw JA, Murray DG, 1973, "Knee Joint Simulator," *Clinical Orthopaedics and Related Research*, **94**, pp. 15-23.
- [5] Swanson SAV, Freeman MAR, Heath JC, 1973, "Laboratory Tests on Total Joint Replacement Prosthese," *The Journal of Bone and Joint Surgery*, **55B**(4), pp. 759-773n
- [6] Zachman NJ, 1977, "Design of a Load Simulator for the Dynamic Evaluation of Prosthetic Knee Joints," M.S. Thesis, Purdue University.
- [7] Pappas MJ, Buechel FF, 1979, "New Jersey knee simulator," *Transactions of the 11th Annual International Biomaterials Symposium*, **3**, pp. 101.
- [8] Rastegar J, Miller N, Barmada R, 1980, "An Apparatus for Measuring the Load-Displacement and Load-Dependent Kinematic Characteristics of Articulating Joints – Application to the Human Ankle Joint," *Journal of Biomechanical Engineering*, **102**, 208-213.
- [9] Treharne RW, Young RW, Young SR, 1981, "Wear of artificial joint materials 3: Simulation of the knee joint using a computer-controlled system," *Engineering in Medicine*, **10**(3), pp. 137-142.
- [10] Ahmed AM, Burke DL, 1983, "In-Vitro Measurements of Static Pressure Distribution in Synovial Joints – Part 1: Tibial Surface of the Knee," *Journal of Biomechanical Engineering*, **105**, pp. 216-225.
- [11] Tong JJ, 1985, "Wrist Motion Simulator," Ph. D. Dissertation, Syracuse University.
- [12] Gillison DB, 1991, "Reconfiguration of the Wrist Joint Motion Simulator," Master's Thesis, Syracuse University.
- [13] Engsberg JR, 1987, "A Biomechanical Analysis of the Talocalcaneal Joint – In Vitro," *Journal of Biomechanics*, **20**(4), pp. 429-442.
- [14] Szklar O, Ahmed AM, 1987, "A Simple Unconstrained Dynamic Knee Simulator," *Journal of Biomechanical Engineering*, **109**, pp. 247-251.
- [15] McLean CA, Ahmed AM, 1993, "Design and Development of an Unconstrained Dynamic Knee Simulator," *Journal of Biomechanical Engineering*, **115**, pp. 144-148.

- [16] Cain PR, Mutschler TA, Fu FH, Lee SK, 1987, "Anterior stability of the glenohumeral joint: A dynamic model," *American Journal of Sports Medicine*, **15**(2), pp. 144-148.
- [17] Lewis JL, Lew WD, Schmidt J, 1988, "Description and Error Evaluation of an In Vitro Knee Joint Testing System," *Journal of Biomechanical Engineering*, **110**, pp. 238-248.
- [18] Berns GS, Hull ML, Patterson HA, 1990, "Implementation of a Five Degree Automated System to Determine Knee Flexibility In Vitro," *Journal of Biomechanical Engineering*, **112**, pp. 392-400.
- [19] Bach JM, Hull ML, 1994, "A New Load Application System for In Vitro Study of Ligamentous Injuries to the Human Knee Joint," 1994 ASME International Mechanical Engineering Congress and Exposition, pp. 1-2.
- [20] DiAngelo D, Schopfer A, Hearn T, Powell J, Tile M, 1992, "Biomechanical Comparison of Internal Fixations of the Posterior Acetabular Column," *ASME Advances in Bioengineering (BED)*, **22**, 577-580.
- [21] King GHW, Itoi E, Risung F, Niebur GL, Morrey BF, An K-N, 1993, "Kinematics and stability of the Norway elbow: A cadaveric study," *Acta Orthopaedica Scandinavica*, **64**(6), pp. 657-663.
- [22] MacWilliams BA, Chao EY, 1994, "Analysis of a Prosthetic Knee System Using a Dynamic Joint Simulator," Thirteenth Southern Biomedical Engineering Conference, pp. 360-363.
- [23] MacWilliams BA, Chao EY, Mejia LC, 1994, "Design and Performance Features of a Knee Dynamic Simulator," Second World Congress of Biomechanics.
- [24] MacWilliams BA, Wilson DR, DesJardins JD, Romero J, Chao EYS, 1999, "Hamstrings Cocontraction Reduces Internal Rotation, Anterior Translation, and Anterior Cruciate Ligament Load in Weight-bearing Flexion," *Journal of Orthopaedic Research*, **17**, pp. 817-822.
- [25] Pavlovic JL, Kirstukas SJ, Touchi H, Bechtold JE, 1994, "Dynamic Simulation Machine for Measurements of Knee Mechanics and Intra-Articular Pressures," *ASME Bioengineering Division*, **28**, pp. 281-282.
- [26] Wuelker N, Wirth CJ, Plitz W, Roetman B, 1995, "A Dynamic Shoulder Model: Reliability Testing and Muscle Force Study," *Journal of Biomechanics*, **28**(5), pp. 489-499.
- [27] Debski RE, McMahon PJ, Thompson WO, Woo SL-Y, Warner JJP, Fu FH, 1995, "A New Dynamic Testing Apparatus to Study Glenohumeral Joint Motion," *Journal of Biomechanics*, **28**(7), pp. 869-874.
- [28] Stroeve S, 1997, "A learning feedback and feedforward neuromuscular control model for two degrees of freedom human arm movements," *Human Movement Science*, **16**, pp. 621-651.
- [29] Werner FW, Palmer AK, Somerset JH, Tong JJ, Gillison DB, Fortino MD, Short WH, 1996, "Wrist Joint Motion Simulator," *Journal of Orthopaedic Research*, **14**, pp. 639-646.
- [30] Walker PS, Blunn GW, Broome DR, Perry J, Watkins A, Sathasivam S, Dewar ME, Paul JP, 1997, "A Knee Simulating Machine for Performance Evaluation of Total Knee Replacements," *Journal of Biomechanics*, **30**(1), pp. 83-89.
- [31] Burgess IC, Kolar M, Cunningham JL, Unsworth A, 1997, "Development of a six station knee wear simulator and preliminary wear results," *Proceedings of the Institution of Mechanical Engineers – Journal of Engineering in Medicine*, **211 Part H**, pp. 37-47.

- [32] Sharkey NA, Hamel AJ, 1998, "A dynamic cadaver model of the stance phase of gait: performance characteristics and kinetic validation," *Clinical Biomechanics*, **13**, 420-433.
- [33] Li G, Rudy TW, Sakane M, Kanamori A, Ma CB, Woo SL-Y, 1998, "The importance of quadriceps and hamstring muscle loading on knee kinematics and in-situ forces in the ACL," *Journal of Biomechanics*, **32**, pp. 395-400.
- [34] Johnson JA, Rath DA, Dunning CE, Roth SE, King GJW, 2000, "Simulation of elbow and forearm motion in vitro using a load controlled testing apparatus," *Journal of Biomechanics*, **33**, pp. 635-639.
- [35] Dunning CE, Duck TR, King GJW, Johnson JA, 2001, "Simulated active control produces repeatable motion pathways of the elbow in an in vitro testing system," *Journal of Biomechanics*, **34**, pp. 1039-1048.
- [36] Dunning CE, Gordon KD, King GJW, Johnson JA, 2003, "Development of a motion-controlled in vitro testing system," *Journal of Orthopaedic Research*, **2003**, pp. 405-411.
- [37] Maletsky LP, Hillbery BM, 2005, "Simulating Dynamic Activities Using a Five-Axis Knee Simulator," *Journal of Biomechanical Engineering*, **127**, pp. 123-133.
- [38] Magnusen JP, 2002, "Design and Fabrication of an Elbow Motion Simulator," Master's Thesis, University of Pittsburgh.
- [39] Kuxhaus L, Schimoler PJ, Viperman JS, Flamm AM, Budny D, Baratz ME, DeMeo PJ, Miller MC, 2007, "Measuring Moment Arms Using Closed-Loop Force Control with an Elbow Simulator," Proceedings of the ASME 2007 Summer Bioengineering Conference.
- [40] Kuxhaus, L, 2008, "Dissertation Title," Ph. D. Dissertation, University of Pittsburgh.
- [41] Popovic RS, 1991, *Hall Effect Devices: Magnetic Sensors and Characterization of Semiconductors*, Adam Hilger, Philadelphia, PA, pp. 55-67, Chapter 3.
- [42] Franklin GF, Powell JD, Workman M, 1998, *Digital Control of Dynamic Systems*, Addison-Wesley, Menlo Park, CA, pp. 66-68, Chapter 3.
- [43] Schimoler PJ, Viperman JS, Kuxhaus L, Flamm AM, Budny DD, Baratz ME, Miller MC, 2007, "Control System for an Elbow Joint Motion Simulator," IMECE2007-42806, ASME IMECE-07 Conference, November 11-15, Seattle, Washington.
- [44] Jacobsen SC, Ko H, Iversen EK, Davis CC, 1990, Control Strategies for Tendon-Driven Manipulators, *Control Systems Magazine*, **10**(2), pp. 23-28.
- [45] Stenerson J, 1999, *Fundamentals of Programmable Logic Controllers, Sensors, and Communications*, Prentice-Hall, Upper Saddle River, New Jersey, pp. 57-94, Chapter 3.
- [46] Skogestad S, Postlethwaite I, 2005, *Multivariable Feedback Control*, John Wiley and Sons, Ltd, Chichester, West Sussex, England, pp. 183, Chapter 5.